ture, and are critical determinants of transcription (3). A tight chromatin structure by histone deacetylation causes transcriptional silencing. Gastric cancer exhibits global histone hypoacetylation and, interestingly, the degree of hypoacetylation is associated with the depth of tumour invasion and with nodal metastases. Hypoacetylation of histones H3 and H4 in the $p21^{WAF1/Cip1}$ promoter region takes place in more than a half of gastric cancers. Hypoacetylation of histone H3 in this promoter is associated with reduced expression of p21, regardless of *p53* gene status (8). Upregulation of histone acetylation in gastric cancer cells by treatment with trichostatin A (a histone deacetylase [HDAC] inhibitor) induces growth arrest, causes apoptosis and suppresses invasion, as the expression of p21, CBP and Bak is induced. In addition to acetylation, phosphorylation and methylation may enhance or inhibit transcription, depending on the residues affected and on the molecules that interact. Histone modification may be a therapeutic target.

MOLECULAR BASES OF GASTRIC AND INTESTINAL PHENOTYPES

In addition to classification by histology (well differentiated and poorly differentiated; intestinal and diffuse), gastric cancers may also be classified into four phenotypes by the mucin expression profile: G-type (gastric or foveolar phenotype), I-type (intestinal phenotype), GI- type (intestinal and gastric mixed phenotype) and N-type (neither gastric nor intestinal phenotype) (4, 9). The G-type is considered to behave more aggressively than the I-type. Mutations of *p53* and LOH of the adenomatous polyposis coli (*APC*) gene occur more frequently in patients with the I-type than with the G-type, while MSI and alterations in the *p73* gene are more common in the G-type than in the I-type. MSI in the G-type is usually associated with inactivation of hMLH1 following promoter hypermethylation. The Caudal-type homeoboxes (CDX) 1 and CDX2 act as intestine-specific transcription factors and are expressed in I-type gastric cancers at high levels. CDX2 upregulates the expression of goblet-specific MUC2 and liver-intestine (LI) cadherin, also known as cadherin 17 (*CDH17*). LI-cadherin expression is more frequently detected in I-type than G-type and is associated with tumour invasion and a poor patient prognosis. On the other hand, the expression of SOX2, a member of transcription factor family containing an *Sry*-like high-mobility group box, is well preserved in the G-type and is downregulated in the I-type.

MOLECULAR EVENTS AND *HELICOBACTER* INFECTION

Recent studies have shed much light on the molecular mechanisms of how *H. pylori* infection is involved in the development of cancer in the stomach (10, 11). Strains of *H. pylori* carrying the cytotoxin-associated antigen A (cagA) gene are associated with the development of gastric cancer. The cagA gene product, CagA, is delivered into gastric epithelial cells by the bacterial type IV secretion system; this induces morphological transformations and cell motility increases. CagA is injected and undergoes tyrosine phosphorylation by Src family kinases, after which it binds to SHP-2 and activates SHP-2 phosphatase. Focal adhesion kinase (FAK) is a tyrosine kinase that plays a critical role in focal adhesion turnover. Activated SHP-2 dephosphorylates and inhibits FAK activity.

Impaired cell adhesion and increased motility by CagA may be involved in the development of gastric lesions associated with *H. pylori* infection. More recently, it has been shown that CagA interacts with cytoplasmic domain of E-cadherin, and competes with beta-catenin binding; this results in accumulation of beta-catenin in both cytoplasm and nucleus. One of the important downstream targets of beta-catenin signaling induced by CagA is CDX1. Forced expression of CagA in gastric epithelial cells induces MUC2 expression. Through this mechanism, CagA may cause intestinal metaplasia which predisposes to gastric cancer, especially of I-type.

GENETIC POLYMORPHISM AND CANCER RISK

An individual's cancer risk varies in line with genetic polymorphisms in the normal population since this connects directly with the person's cancer prevention. Most genetic polymorphism between individuals is due to single nucleotide polymorphisms (SNPs). Genetic polymorphism is crucial for various processes related to gastric carcinogenesis, including 1) the mucosal protection and inflammatory response against *H. pylori* infection; 2) the functioning of carcinogen detoxification and antioxidant protection; 3) the intrinsic variability of DNA repair processes; and 4) cell proliferation activity (4, 12). Variants of IL-1beta (*IL1B*) and IL-1 receptor antagonist (*IL1RN*) genes, *IL1B* (–31 T genotype) and *IL1RN* IVS 86bp VNTR (2/2 genotype) increase IL-1beta production and inhibit gastric acid secretion. This is associated with a risk of a chronic hypochlorhydric response to *H. pylori* infection and an increased gastric cancer risk. *NAT1* is responsible for N-acetyltransferase activity which catalyses acetylation and modification of aromatic and heterocyclic amine carcinogens. A significantly increased risk of gastric cancer is associated with certain genotypes of NAT1 (1088 T>A, 1095 C>A).

SNPs are present in the transmembrane domain of *HER-2/c-erb*B2 (655 Ile>Val, A>G) and in the promoter regions of *EGF* (61 A/G) and *MMP-9* (–1562 C/T). SNPs of *HER-2* and *EGF* significantly affect the risk of gastric cancer, while the genotype of *MMP-9* does not; it is, however, associated with tumour invasion, metastasis and tumour stage (5). Importantly, genetic polymorphisms are also associated with therapeutic efficacy and the toxicity of anti-cancer drugs. VNTR polymorphism in the promoter region of the thymidylate synthase gene influences the response to 5-fluorouracil (5-FU). The number of TA repeats in the promoter region of the UDP-glucuronosyltrans-

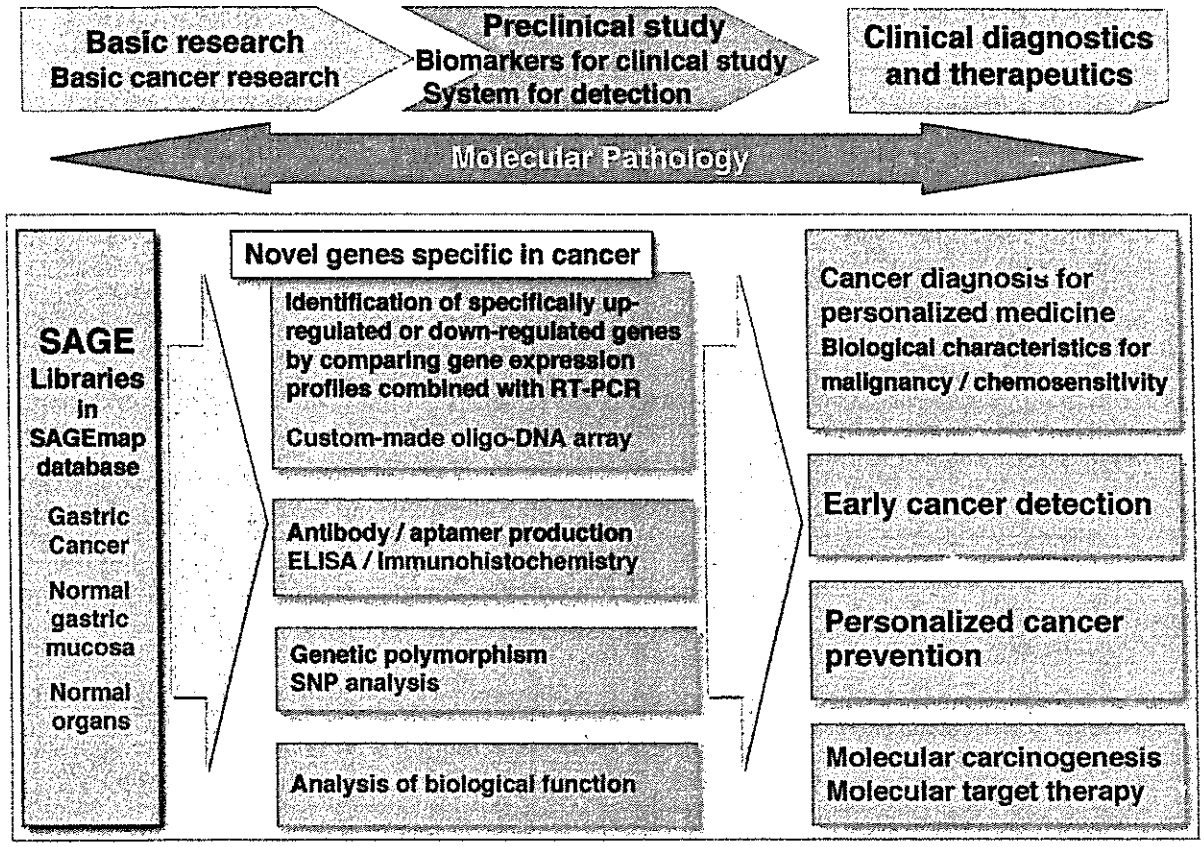

Fig. 2. Strategy to search for novel genes of gastric cancer through gene expression profiles; clinical implications.

ferase 1A1 gene affects the degree of toxicity during irinotecan therapy.

SEARCH FOR NOVEL GENES INVOLVED IN GASTRIC CARCINOGENESIS

Thus, gastric cancer is accompanied by several genetic and epigenetic alterations: mutations, gene amplifications, LOH, gene silencings by DNA methylation and losses of imprinting. All of these alterations modify gene expression. Therefore, genome-wide studies of gene expression are extremely important for studying the precise mechanisms of cancer emergence and progression. In addition to the microarray technique, the Serial Analysis of Gene Expression (SAGE) technique is a powerful tool to allow genome-wide, quantitative analysis of gene expression with high reproducibility (6). Fig. 2 shows a strategy of clinical applications of SAGE with regard to diagnostics, treatment and prevention.

We have created the largest SAGE library of gastric cancer in the world. It contains a total of 137,706 expressed tags including 38,903 unique tags (GEO accession number GSE 545) (*Internet address: http://www.ncbi.nlm.nih.gov/SAGE/*) (4, 13). The library is built on 5 samples of gastric cancer with different histology and stage. We have found that *APOC1*, *CEACAM6*, and *YF13H12* are often overexpressed in gastric cancer, while *FUS*, *CDH17*, *COL1A1*, *COL1A2*, and *APOE* are associated with tumour progression according to studies where we have compared SAGE libraries between gastric cancers and healthy gastric mucosa in combination with quantitative RT-PCR. Tumours that are LI-cadherin (*CDH17*)-positive by immunostaining are often diagnosed only at a late stage, and the prognosis of patients with LI-cadherin-positive tumours is worse than with negative tumours.

In a search for gastric cancer-specific genes, we compared gastric cancer SAGE libraries with various healthy tissues of crucial organs in the SAGE-map database, and identified 54 candidate genes (14). Quantitative RT-PCR analysis revealed that *APIN*, *TRAG3*, *CYP2W1*, *MIA*, *MMP-10*, *DKK4*, *GW112*, *REGIV*, and *HORMAD1* are expressed much more strongly in gastric cancers than in healthy samples of 14 crucial organs. Immunostaining of MIA (melanoma inhibitory activity) and MMP-10 correlated with a poor prognosis in patients who had advanced gastric cancer. According to enzyme-linked immunosorbent assay (ELISA) there were high levels of MMP-10 in most serum samples (95%) from patients with gastric cancer. MIA-transfected gastric cancer cells were up to three times more invasive than cells transfected with empty vector. Therefore, MMP-10 is a good serum marker for gastric cancer, while MIA and MMP-

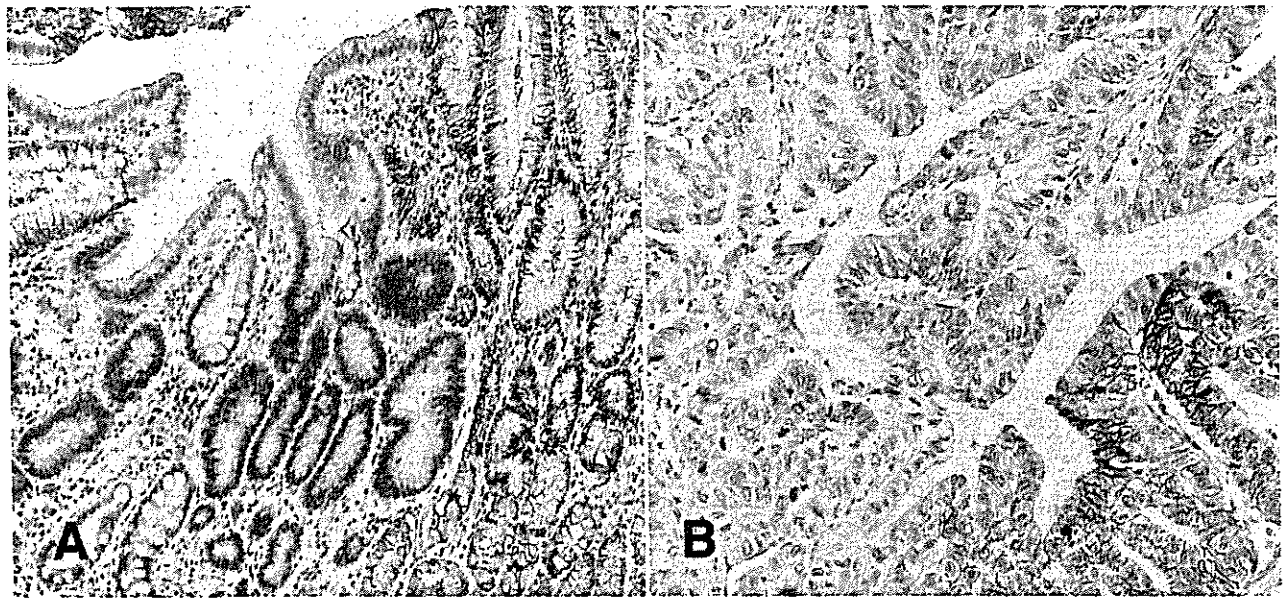

Fig. 3. Reduced expression of claudin-18 in intestinal metaplasia, adenoma and adenocarcinoma of the stomach. Normal gastric epithelial cells express uniformly claudin-18 along with the cell membrane, but there is an obvious reduction of claudin-18 expression in adenoma and adjacent intestinal metaplasia (A) and adenocarcinoma (B) of the stomach.

10 are prognostic factors for gastric cancer patients. Since expression of MIA and MMP-10 is so closely restricted in cancer, these two molecules might also turn out to be good and nontoxic therapeutic targets.

Regenerating islet-derived family member 4 (RegIV) belongs to a superfamily of calcium-dependent lectins. RegIV-positive tissue is associated with the intestinal mucin phenotype as well as with neuroendocrine differentiation of gastric cancer (15). RegIV is also expressed in colorectal carcinomas, carcinoids and pancreatic cancers, but not in lung and breast cancers. High and specific levels of RegIV are detected in 36% of serum samples by ELISA from gastric cancer patients. *In vitro* studies with RegIV-transfected cells have shown that RegIV inhibits 5-FU induced apoptosis through induction of EGFR phosphorylation and inhibition of caspase-3 and -9. Expression of RegIV is strongly associated with resistance to combination chemotherapy with 5-FU and cisplatin. These findings suggest that RegIV may serve as a novel biomarker and an indicator of chemoresistance of gastric cancer.

In an effort to search for novel tumour suppressor genes in gastric cancer, genes with a decreased expression in gastric cancer tissue were screened by SAGE data analysis and RT PCR; *CLDN18* (encoding claudin-18) was down-regulated in gastric cancer (16). The claudin protein family comprises 24 members (claudin-1 to claudin-24) that are important components of tight junction strands in polarised epithelial cells, including gastric epithelia. Expression of claudin-18 is reduced in some instances of intestinal metaplasia, and many gastric adenomas and carcinomas (Fig. 3). Downregulation of claudin-18 was correlated with poor survival in advanced gastric cancers. Down-regulation of claudin-18 was observed in over 70% of gastric cancers with intestinal mucin phenotype. Downregulation of claudin-18 may be an early event in gastric carcinogenesis and constitutes also a good marker of poor survival of gastric cancer patients. SAGE-based analyses thus provide a list of candidate genes that are involved in gastric carcinogenesis and may serve as novel diagnostic markers and therapeutic targets in our strive to combat gastric cancer.

CONCLUSION

Molecular events during gastric carcinogenesis and a search for novel genes through global analysis of gene expression were described. Advances in our understanding the genetic and molecular bases of cancer lead to new diagnosis and therapy. Decision of cancer treatment may be guided by the molecular attributes of the individual patient. It is said that cancer treatment gets personal (17).

REFERENCES

1. Yasui W, Oue N, Kuniyasu H, Ito R, Tahara E, Yokozaki H: Molecular diagnosis of gastric cancer: present and future. Gastric Cancer 2001;4:113–121
2. Yokozaki H, Yasui W, Tahara E: Genetic and epigenetic changes in stomach cancer. Int Rev Cytol 2001;204:49–95
3. Yasui W, Oue N, Ono S, Mitani Y, Ito R, Nakayama H: Histone acetylation and gastrointestinal carcinogenesis. Ann NY Acad Sci 2003;983:220–231
4. Yasui W, Oue N, Kitadai Y, Nakayama H: Recent advances in molecular pathobiology of gastric carcinoma. In: The diversity

of gastric carcinoma. Eds M. Kaminishi, K. Takubo and K. Mafune. Springer-Verlag, Tokyo, 2005, pp. 51–71
5. Yasui W, Oue N, Aung PP, Matsumura S, Shutoh M, Nakayama H: Molecular-pathological prognostic factors of gastric cancer: a review. Gastric Cancer 2005;8:86–94
6. Yasui W, Oue N, Ito R, Kuraoka K, Nakayama H: Search for new biomarkers of gastric cancer through serial analysis of gene expression and its clinical implications. Cancer Sci 2004;95:385–392
7. Oue N, Mitani Y, Motoshita J, Matsumura S, Yoshida K, Kuniyasu H, Nakayama H, Yasui W: Accumulation of DNA methylation is associated with tumor stage in gastric cancer. Cancer 2006;106:1250–1259
8. Mitani Y, Oue N, Hamai Y, Aung PP, Matsumura S, Nakayama H, Kamata N, Yasui W: Histone H3 acetylation is associated with reduced $p21^{WAF1/CIP1}$ expression in gastric carcinoma. J Pathol 2005;205:65–73
9. Tatematsu M, Tsukamoto T, Inada K: Stem cells and gastric cancer: role of gastric and intestinal mixed intestinal metaplasia. Cancer Sci 2003;94:135–141
10. Hatakeyama M: Oncogenic mechanisms of the Helicobacter pylori CagA protein. Nature Rev Cancer 2004;4:688–694
11. Tsutsumi R, Takahashi A, Azuma T, Higashi H, Hatakeyama M: Focal adhesion kinase is a substrate and downstream effector of SHP-1 complexed with Helicobacter pylori CagA. Mol Cell Biol 2006;26:261–276
12. Gonzalez CA, Sala N, Capella G: Genetic susceptibility and gastric cancer risk. Int J Cancer 2002;100: 249–260
13. Oue N, Hamai Y, Mitani Y, Matsumura S, Oshimo Y, Aung PP, Kuraoka K, Nakayama H, Yasui W: Gene expression profile of gastric carcinoma; identification of genes and tags potentially involved in invasion, metastasis, and carcinogenesis by serial analysis of gene expression. Cancer Res 2004;64:2397–2405
14. Aung PP, Oue N, Mitani Y, Nakayama H, Koshida K, Noguchi T, Bosserhoff AK, Yasui W: Systematic search for gastric cancer-specific genes based on SAGE data: melanoma inhibitory activity and matrix metalloproteinase-10 are novel prognostic factors in patients with gastric cancer. Oncogene 2006;25:2546–2557
15. Oue N, Mitani Y, Aung PP, Sakakura C, Takeshima Y, Kaneko M, Noguchi T, Nakayama H, Yasui W: Expression and localization of Reg IV in human neoplastic and non-neoplastic tissues: Reg IV expression is associated with intestinal and neuroendocrine differentiation in gastric adenocarcinoma. J Pathol 2005;207:185–198
16. Sanada Y, Oue N, Mitani Y, Yoshida K, Nakayama H, Yasui W: Down-regulation of the claudin-18 gene, identified through serial analysis of gene expression data analysis, in gastric cancer with an intestinal phenotype. J Pathol 2006;208:633–642
17. Varmus H: The new era in cancer research. Science 2006;312: 1162–1165

Received: September 1, 2006

Expression of Wnt-5a Is Correlated with Aggressiveness of Gastric Cancer by Stimulating Cell Migration and Invasion

Manabu Kurayoshi,[1,2] Naohide Oue,[3] Hideki Yamamoto,[1] Michiko Kishida,[1] Atsuko Inoue,[4] Toshimasa Asahara,[2] Wataru Yasui,[3] and Akira Kikuchi[1]

Departments of [1]Biochemistry, [2]Surgery, [3]Molecular Pathology, and [4]Pharmacology, Graduate School of Biomedical Sciences, Hiroshima University, Hiroshima, Japan

Abstract

Wnt-5a is a representative ligand that activates a β-catenin-independent pathway in the Wnt signaling. Although abnormal activation of β-catenin-dependent pathway is often observed in human cancer, the relationship between β-catenin-independent pathway and tumorigenesis is not clear. We sought to clarify how Wnt-5a is involved in aggressiveness of gastric cancer. Abnormal expression of Wnt-5a was observed in 71 of 237 gastric cancer cases by means of immunohistochemistry. The positivity of Wnt-5a expression was correlated with advanced stages and poor prognosis of gastric cancer. Wnt-5a had the abilities to stimulate cell migration and invasion in gastric cancer cells. Wnt-5a activated focal adhesion kinase and small GTP-binding protein Rac, both of which are known to play a role in cell migration. Cell migration, membrane ruffling, and turnover of paxillin were suppressed in Wnt-5a knockdown cells. Furthermore, anti-Wnt-5a antibody suppressed gastric cancer cell migration. These results suggest that Wnt-5a stimulates cell migration by regulating focal adhesion complexes and that Wnt-5a is not only a prognostic factor but also a good therapeutic target for gastric cancer. (Cancer Res 2006; 66(21): 10439-48)

Introduction

Wnt proteins are a large family of cysteine-rich secreted molecules (1). At least 19 Wnt members are present in mammals to date. The members exhibit unique expression patterns and distinct functions in development. The Wnt family members can be divided into three distinct types based on their ability to induce transformation of the mouse mammary epithelial cell line C57MG (2, 3). The highly transforming members include Wnt-1, Wnt-3a, and Wnt-7a. The intermediately transforming members include Wnt-2, Wnt-5b, and Wnt-7b and nontransforming members are Wnt-4, Wnt-5a, Wnt-6, and Wnt-11.

The intracellular signaling pathway activated by Wnt proteins was originally identified as a β-catenin-dependent signaling pathway that is highly conserved among species (1). According to the most widely accepted current model of the β-catenin pathway, in the absence of Wnt, β-catenin is phosphorylated and ubiquitinated in the Axin complex, resulting in the degradation of β-catenin by the proteasome (4–7). Consequently, the cytoplasmic β-catenin level is low. When Wnt acts on its cell surface receptor consisting of Frizzled and lipoprotein receptor-related protein 5/6, β-catenin escapes from degradation in the Axin complex (8). The accumulated β-catenin is translocated to the nucleus, where it binds to the transcription factor T-cell factor (Tcf)/lymphoid enhancer factor (Lef) and thereby stimulates the expression of various genes (9). It is thought that the Wnt proteins showing the high transforming activity in C57MG cells activate the β-catenin pathway.

Some Wnt proteins activate a β-catenin-independent pathway that primarily modulates cell movement and polarity (3, 10). There are at least three mechanisms, which overlap with other signaling pathways. First, specific Wnt and Frizzled can activate calcium/calmodulin-dependent protein kinase II and protein kinase C (PKC). Second, some Frizzled receptors act through heterotrimeric G proteins to activate phospholipase C and phosphodiesterase. Lastly, the planar cell polarity pathway in *Drosphila* is mediated by Frizzled, which activates Rac, Rho, c-Jun NH_2-terminal kinase (JNK), and Rho-associated kinase. It is generally believed that the intermediately transforming and nontransforming Wnt proteins activate the β-catenin-independent pathway (3).

Wnt-5a is a representative of Wnt proteins that activate the β-catenin-independent pathway. Some reports indicate that Wnt-5a acts as a tumor suppressor because Wnt-5a has an ability to inhibit the β-catenin pathway. For instance, Wnt-5a has been shown to induce the down-regulation of β-catenin through Siah2 (11) or to inhibit the transcriptional activity of Tcf/Lef (12, 13). Antisense Wnt-5a mimics Wnt-1-mediated C57MG cell transformation (14). Wnt-5a negatively regulates B-cell proliferation, and Wnt-5a heterozygous mice develop B-cell lymphoma (15). Furthermore, Wnt-5a inhibits proliferation, migration, and invasiveness in thyroid tumor and colorectal cancer cell lines (16, 17). In contrast to these observations, it has also been suggested that Wnt-5a has oncogenic properties based on the findings that the Wnt-5a mRNA level is up-regulated in lung cancers, prostate cancers, and breast cancers (18). There is a correlation between Wnt-5a expression and increased cell motility and invasiveness in melanoma cells and breast cancer cells with tumor-associated macrophages (19, 20). Thus, the functions of Wnt-5a in human cancers are controversial and still unclear.

According to the WHO, gastric cancer is the fourth most common malignancy worldwide, with ~870,000 new cases occurring yearly (21). However, the relationship between the expression of Wnt-5a and aggressiveness of gastric cancer is not known. In this study, we found that the Wnt-5a protein is highly expressed in advanced stages of gastric cancer and that its expression is correlated with poor prognosis. Furthermore, we showed that Wnt-5a stimulates cell migration and invasion of gastric cancer cells through regulating focal adhesion complexes.

Requests for reprints: Akira Kikuchi, Department of Biochemistry, Graduate School of Biomedical Sciences, Hiroshima University, 1-2-3 Kasumi, Minami-ku, Hiroshima 734-8551, Japan. Phone: 81-82-257-5130; Fax: 81-82-257-5134; E-mail: akikuchi@hiroshima-u.ac.jp.

doi:10.1158/0008-5472.CAN-06-2359

Materials and Methods

Materials and chemicals. TOP-*fos*-Luc, pUC/EF-1α/β-catenin$^{S\text{-}A}$, and pCMV-sFRP2-Flag were provided by Drs. H. Clevers (University Medical Center, Utrecht, the Netherlands), A. Nagafuchi (Kumamoto University, Kumamoto, Japan), and T. Akiyama (Tokyo University, Tokyo, Japan), respectively. pEGFP-Paxillin and pGEX-αPAK-CRIB were provided by Drs. H. Sabe (Osaka Bioscience Institute, Osaka, Japan) and K. Kaibuchi (Nagoya University, Nagoya, Japan), respectively. Two anti-Wnt-5a antibodies were generated in rabbits by immunization with synthetic peptides corresponding to residues 165 to 181 and residues 275 to 290 of human Wnt-5a. The former antibody recognized both Wnt-5a and Wnt-5b, whereas the latter reacted with Wnt-5a only. Wnt-5a was purified to near homogeneity by the similar procedures to the purification of Wnt-3a (22). The details of the purification of Wnt-5a will be described elsewhere. Secreted Frizzled-related protein 2 (sFRP2) conditioned medium was prepared from culture medium of HEK293T cells stably expressing sFRP2. The cells were seeded at a density of 1×10^6/mL in DMEM/Ham's F-12 supplemented with 10% fetal bovine serum (FBS). At 24 hours after plating, the medium was replaced with Opti-MEM medium (Life Technologies, Minneapolis, MN), and then 3 days after, sFRP2 conditioned medium was collected. Anti-Wnt-3a antibody was prepared as described (22). MKN-45 and MKN-1 cells were grown in RPMI 1640 supplemented with 10% FBS. MKN-45 cells stably expressing mouse Wnt-5a were generated by selection with G418. MKN-1 cells stably expressing green fluorescent protein (GFP)-paxillin were generated by selection with puromycin. In analyses with small interfering RNA (siRNA) for Wnt-5a, the human Wnt-5a mRNA target sequences, 5′-CTGTGGATAACACCTCTGTTT-3′ and 5′-AAA-AACAGAGGTGTTATCCAC-3′, were used. Scrambled siRNA, 5′-CAGTCGC-GTTTGCGACTGG-3′, was used as a control. Anti-Wnt-4, anti-HK-ATPase, and anti-chromogranin A antibodies were obtained from R&D Systems (Minneapolis, MN), Affinity Bioreagents (Golden, CO), and Novocastra (Newcastle, United Kingdom), respectively. Other materials were obtained from commercial sources.

Tissue samples. In all, 250 primary tumors were collected from patients diagnosed with gastric cancer. Patients were treated at the Hiroshima University Hospital (Hiroshima, Japan) or an affiliated hospital. For quantitative reverse transcription-PCR (RT-PCR), 13 gastric cancer samples and corresponding nonneoplastic mucosa samples were used. For immunohistochemical analysis, archival formalin-fixed, paraffin-embedded tissues from 237 patients who had undergone surgical excision for gastric cancer were used. Histologic classification (intestinal, diffuse-adherent, and diffuse-scattered types) was made according to the Lauren classification system (23, 24). Tumor staging was according to the tumor-node-metastasis staging system. The procedure to protect privacy was in accordance with the Ethical Guidelines for Human Genome/Gene Research enacted by the Japanese Government.

Immunohistochemistry and immunocytochemistry. The samples were sectioned, deparaffinized, and stained with H&E to ensure that the sectioned block contained tumor cells. Adjacent sections were then immunohistochemically stained. For immunostaining of Wnt-5a, a DAKO CSA kit (DAKO, Carpinteria, CA) was used according to the manufacturer's recommendations. In brief, sections were pretreated by microwaving in citrate buffer for 30 minutes to retrieve antigenicity. After peroxidase activity was blocked with 3% H_2O_2-methanol for 10 minutes, sections were incubated with normal goat serum (DAKO) for 20 minutes to block nonspecific antibody binding sites. Anti-Wnt-5a antibody was incubated with tissue samples for 15 minutes at room temperature and detected by incubating for 15 minutes with biotinylated goat anti-rabbit immunoglobulins, and the signal was amplified and visualized by the substrate-chromogen solution. The sections were counterstained with 0.1% hematoxylin. The staining for Wnt-5a, Wnt-3a, or Wnt-4 was classified according to the percentage of stained cancer cells. Expression was considered to be "negative" if <50% (0, 0-10%; 1+, 10-50%) of cancer cells were stained. When at least 50% (2+, 50-80%; 3+, >80%) of cancer cells were stained, the immunostaining was considered "positive."

The immunostaining of β-catenin, HK-ATPase, chromogranin A, epidermal growth factor receptor (EGFR), melanoma inhibitory activity (MIA), and matrix metalloproteinase-10 (MMP-10) was basically done as described previously (25). The immunocytochemical analyses of the cultured cells were done as described (26, 27).

Statistical analyses. Statistical analyses for Table 1 were carried out with Fisher's exact test. Kaplan-Meier survival curves were constructed for patients positive and negative with Wnt-5a, β-catenin, EGFR, MIA, or MMP-10. Differences between survival curves in Fig. 5 were tested for statistical significance by log-rank test. $P < 0.05$ was considered statistically significant.

Cell migration and invasion assays. To measure the cell migration activity, Transwell assays were done using a modified Boyden chamber (tissue culture treated, 6.5 mm in diameter, 10-μm thick, 8-μm pores; Transwell, Costar, Cambridge, MA) as described (27). The lower surface of filters was coated with 10 μg/mL collagen. MKN-1, MKN-7, MKN-74, and MKN-45 cells (2.5×10^4 cells in 100 μL) suspended in serum-free RPMI 1640 containing 0.1% bovine serum albumin were applied to the upper chamber. The same medium was added to the lower chamber. When necessary, 600 ng/mL Wnt-5a was added to the lower chamber. After the cells were incubated at 37°C for 4 to 8 hours, the number of cells that migrated to the lower side of the upper chamber was counted. The invasive potential of the cells was analyzed using a Matrigel-coated modified Boyden chamber (Becton Dickinson, Bedford, MA). RPMI 1640 containing 10% FBS was added to the lower chamber. After incubation at 37°C for 24 hours, the number of cells that migrated to the lower side of the upper chamber was counted.

To carry out the wound healing assay, the cells were plated onto collagen-coated coverslips. The monolayer MKN-1 cells were then scratched manually with a plastic pipette tip, and after being washed with PBS, the wounded monolayers of the cells were allowed to heal for 6 to 12 hours in RPMI 1640 containing 10% FBS (27). When necessary, conditioned medium containing sFRP2 or anti-Wnt-5a antibody (50 μg/mL) was added to the medium.

Table 1. Relationship between Wnt-5a expression and clinicopathologic characteristics in gastric cancer

	Wnt-5a expression		*P*
	Positive, *n* (%)	Negative, *n*	
T grade			
T_1	5 (7.6)	61	<0.0001
$T_2/T_3/T_4$	66 (38.6)	105	
N grade			
N_0	15 (14.2)	91	<0.0001
$N_1/N_2/N_3$	56 (42.7)	75	
Stage			
I/II	18 (13.8)	112	<0.0001
III/IV	53 (49.5)	54	
Histologic type			
Diffuse-scattered	32 (59.3)	22	<0.0001
Other	39 (21.3)	144	
β-Catenin nuclear/cytoplasmic accumulation			
Positive	9 (18.0)	41	0.0386
Negative	62 (33.2)	125	

NOTE: T_1, tumor invades lamina propria or submucosa; T_2, tumor invades muscularis propria or subserosa; T_3, tumor penetrates serosa without invasion of adjacent structures; and T_4 tumor invades adjacent structures. N_0, no regional lymph node metastasis; N_1, metastasis in 1 to 6 regional lymph nodes; N_2, metastasis in 7 to 15 regional lymph nodes; and N_3, metastasis in >15 regional lymph nodes.

Cell proliferation assay. Cells were seeded at a density of 1.0×10^5/mL. At 12 hours after plating, the medium was replaced with 2% serum medium. The cell number was counted every 24 hours for 4 days.

Live imaging of focal adhesion. The dynamics of GFP-paxillin of the scattered monolayer cells were quantitated as described previously (27). Fluorescence intensities of individual adhesions from background-subtracted images were measured over time using MetaMorph software (Universal Imaging Corp., Downingtown, PA).

Others. Semiquantitative RT-PCR was done as described (28). Forward and reverse primers were as follows: Wnt-5a, 5′-CTTCGCCCAGGTTG-TAATTGAAGC-3′ and 5′-CTGCCAAAAACAGAGGTGTTATCC-3′; Wnt-5b, 5′-AGGGAACCCTACTCTGG-3′ and 5′-ACATCTCGGGTCTCTG-3′; and ribosomal high basic 23-kDa protein (RPL), GACCGTCTCAAGGTGT and CTT-CCGGTAGTGGATCT. Tcf-4 transcriptional activity was measured as described (26, 29). Cell adhesion assay was done by placing the cells on collagen-precoated dishes (27). Activation of Rac was assayed using glutathione *S*-transferase (GST)-CRIB (27).

Results

Expression of Wnt-5a in gastric cancer. There are two Wnt-5 family members, Wnt-5a and Wnt-5b, and they share 90% amino acid identity. The medium mRNA levels of Wnt-5a in the nontumor and tumor regions in the stomach of 13 gastric cancer patients were 3.6- and 11.6-fold higher than those of Wnt-5b (Fig. 1*A*). The median mRNA level of Wnt-5a in gastric cancer samples was up-regulated 2.6-fold ($P < 0.05$, Wilcoxon test) compared with that in corresponding nontumor mucosa samples, whereas the mRNA level of Wnt-5b showed no significant differences between gastric cancer and corresponding nontumor mucosa of individuals (Fig. 1*A*).

To evaluate where Wnt-5a protein is expressed in the normal gastric mucosa and which type of gastric cancer exhibits Wnt-5a expression, we did immunohistochemistry. Anti-Wnt-5a antibody specifically recognized Wnt-5a in the lysates of L cells expressing Wnt-5a (Fig. 1*B*). This anti-Wnt-5a antibody did not recognize Wnt-3a, Wnt-4, Wnt-7a, or Wnt-11 (data not shown). Immunohistochemical staining revealed the presence of Wnt-5a at the base of the normal gastric corpus mucosa (Fig. 1*C, a*). Weak or no staining of Wnt-5a was observed in foveolar epithelium and stromal cells. Wnt-5a-positive cells were negative for HK-ATPase (a marker of parietal cells) and chromogranin A (a marker of endocrine cells), indicating that Wnt-5a-positive cells were the Chief cells (Fig. 1*C, b* and *c*). This staining was not observed when anti-Wnt-5a antibody was preincubated with a peptide corresponding to a portion of Wnt-5a (data not shown).

Next, we did immunohistochemical staining of Wnt-5a in 237 human gastric cancer cases. Representative results of Wnt-5a immunostaining of gastric cancer are shown in Fig. 1*C, d* and *e*. Wnt-5a was detected in cancer cells in both intestinal-type and diffuse-type (diffuse-adherent and diffuse-scattered) gastric cancer. Although it is difficult to distinguish diffuse-scattered-type gastric cancer cells from stromal cells, CAM5.2 (a marker for epithelial cell)–positive cells were positive for Wnt-5a (Fig. 1*C, f*). These results indicate that Wnt-5a is expressed in epithelial-derived cancer cells.

Among 237 gastric cancer cases, expression of Wnt-5a was observed in 71 (30.0%) cases. Positivity for Wnt-5a was associated with advanced T grade (depth of invasion) and N grade (degree of lymph node metastasis; $P < 0.0001$ and $P < 0.0001$, respectively; Table 1). Moreover, Wnt-5a staining was observed more frequently in stage III/IV cases [53 of 107 (49.5%) cases] than in stage I/II cases [18 of 130 (13.8%) cases; $P < 0.0001$; Table 1]. When all the cases were classified into diffuse-scattered type and other types (intestinal type and diffuse-adherent type), Wnt-5a was more frequently expressed in diffuse-scattered-type gastric cancer [32 of 54 (59.3%) cases] than in other types of gastric cancer [39 of 183 (21.3%) cases; $P < 0.0001$; Table 1]. We generated two antibodies against Wnt-5a, and analyses with the different antibodies produced almost the same results. In contrast, the immunohistochemical analyses using anti-Wnt-3a or anti-Wnt-4 antibody revealed that these gastric cancer cases show heterogeneity of weak staining for Wnt-3a or Wnt-4 and that the positivity of the expression of these Wnt proteins does not associate with aggressiveness of gastric cancer (data not shown). These findings suggest that highly expressed Wnt-5a could be generally related to tumor progression of gastric cancer.

It has been reported that adenomatous polyposis coli (APC) or β-catenin gene mutations are detected in gastric cancer (30). Cytosomal or nuclear accumulation of β-catenin was observed in 50 (21.1%) cases of 237 gastric cancer cases. Among the 50 gastric cancer cases with cytosomal or nuclear accumulation of β-catenin, only 9 gastric cancer cases showed Wnt-5a expression (Table 1). However, Wnt-5a and β-catenin were rarely expressed in the same gastric cancer cells. In the nine gastric cancer cases with positive Wnt-5a expression, none of β-catenin-positive cancer cells showed the abnormal expression of Wnt-5a (Fig. 1*D, a* and *b*), except for one gastric cancer case. These findings suggest that β-catenin and Wnt-5a are expressed exclusively in gastric cancer.

Actions of Wnt-5a on cell growth and migration of gastric cancer cells. Comparison of various gastric cancer cell lines revealed that the expression level of Wnt-5a mRNA in MKN-1, MKN-7, and MKN-74 cells is higher than that of TMK-1, MKN-28, MKN-45, HSC-39, and KATO-III cells (Fig. 2*A, a*). The genes of APC and β-catenin in these cells are not mutated, except for MKN-28 and HSC-39 cells (31). It has been reported that Wnt-5a suppresses the transcriptional activity of Tcf/Lef by acting downstream of β-catenin (12, 13) or is involved in cell migration (19, 20). Ectopic expression of β-catenin in MKN-45 cells activated Tcf-4, and this β-catenin-dependent transcriptional activity was indeed decreased by purified Wnt-5a protein (Fig. 2*A, b*). However, expression of Wnt-5a in MKN-45 cells did not affect cell growth (Fig. 2*A, c*). These results suggest that Wnt-5a does not have an influence on cell proliferation in gastric cancer cells where β-catenin is not abnormally expressed. Therefore, we asked whether Wnt-5a is involved in migration activity of gastric cancer.

The migration activities in MKN-1 and MKN-7 cells were higher than those of MKN-74 and MKN-45 cells (Fig. 2*B, a*). Because it seemed that the migration activity in the cell lines has a tendency to be dependent on the expression levels of Wnt-5a, we used MKN-1 and MKN-45 cells in the following experiments. Expression of Wnt-5a in MKN-45 cells stimulated the cell migration (Fig. 2*B, b*), and knockdown of Wnt-5a by RNA interference in MKN-1 cells suppressed the migration (Fig. 2*B, c*). Furthermore, whereas control MKN-1 cells invaded the Matrigel, Wnt-5a knockdown MKN-1 cells were less invasive (Fig. 2*B, d*).

sFRP2 binds to Wnt proteins and acts as a negative regulator of Wnt signaling (32). MKN-1 cells were allowed to migrate in scratch-wound cultures, resulting in wound closure after 6 hours, and the migration of MKN-1 cells in scratch-wound cultures was inhibited by the addition of sFRP2 conditioned medium (Fig. 2*C*). Furthermore, anti-Wnt-5a antibody suppressed the migration of MKN-1 cells in scratch-wound cultures (Fig. 2*D, a* and *b*). The inhibitory activity of this antibody for Wnt-5a was confirmed by

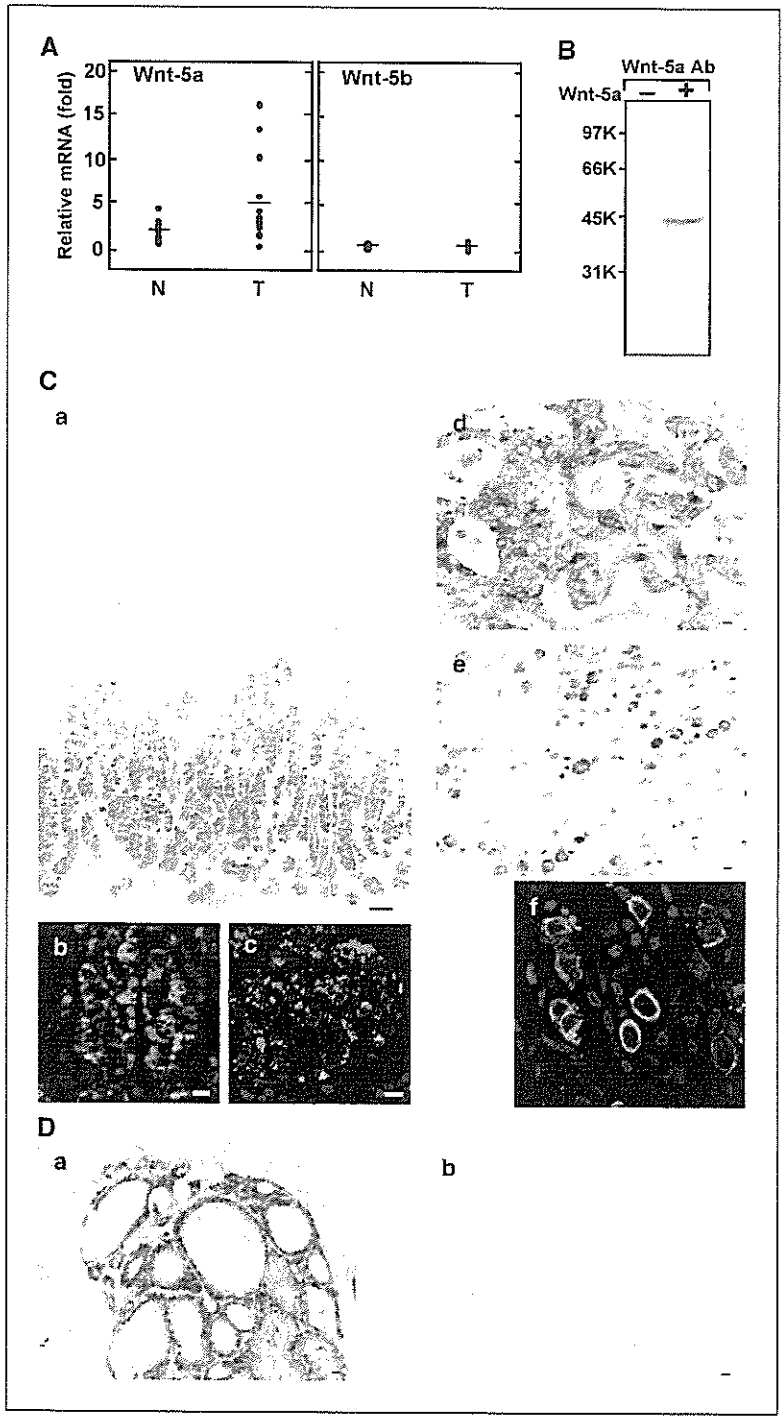

Figure 1. Expression of mRNA and proteins of Wnt-5a in nontumor and tumor regions of human stomach. *A*, expression of mRNA of Wnt-5a and Wnt-5b in normal stomach and gastric cancer. RT-PCR was used to quantitatively amplify mRNA of Wnt-5a, Wnt-5b, and RPL from tumor (*T*) and adjacent nontumor (*N*) regions in 13 individuals. The mRNA levels of Wnt-5a (*left*) and Wnt-5b (*right*) are presented as arbitrary units for the mRNA levels of RPL. *B*, specificity of anti-Wnt-5a antibody. The lysates of control L cells and L cells expressing Wnt-5a were probed with anti-Wnt-5a antibody. *C*, expression of Wnt-5a in gastric cancer. *a*, normal human stomach was immunostained with anti-Wnt-5a antibody (*brown*). Bar, 100 μm. *b* and *c*, the samples was stained with anti-Wnt-5a antibody (*red*) and anti-HK-ATPase (*b*) or chromogranin A (*c*) antibody (*green*). Nuclei were shown by 4′,6-diamidino-2-phenylindole (DAPI; *blue*). Bar, 10 μm. *d*, intestinal-type gastric cancer was immunostained with anti-Wnt-5a antibody. Bar, 20 μm. *e*, diffuse-scattered-type gastric cancer was immunostained with anti-Wnt-5a antibody. Bar, 20 μm. *f*, diffuse-scattered-type gastric cancer was stained with anti-Wnt 5a antibody (*red*), anti-CAM5.2 (*green*; a marker for epithelial cell) antibody, and DAPI (*blue*). Bar, 10 μm. *D*, expression of β-catenin in gastric cancer. A sample of gastric cancer was stained with anti-β-catenin (*a*) and anti-Wnt-5a (*b*) antibodies. Bar, 40 μm.

another way. Wnt-5a has been shown to induce the phosphorylation of Dvl (33). Preincubation of Wnt-5a and anti-Wnt-5a antibody inhibited Wnt-5a-dependent phosphorylation of Dvl (Fig. 2*D*, *c*). These results indicate that Wnt-5a stimulates cell migration and invasion in the gastric cancer cells.

Molecular mechanism by which Wnt-5a stimulates cell migration. Expression of Wnt-5a in MKN-45 cells increased cell adhesiveness (Fig. 3*A*), suggesting that Wnt-5a enhances signaling from focal adhesions. Activation of focal adhesion kinase (FAK) and small GTP-binding protein Rac is necessary for cell migration (34). FAK is activated via autophosphorylation at Tyr^{397}, which is initiated by integrin engagement with its ligand (34). Adhesion-dependent FAK activation was enhanced by expression of Wnt-5a in MKN-45 cells (Fig. 3*B*). Addition of purified Wnt-5a protein to MKN-45 cells activated FAK and Rac within 5 minutes (Fig. 3*C*). Treatment of the cells with PP2, a Src inhibitor, and GF109203X, a PKC inhibitor, suppressed Wnt-5a-dependent FAK activation as well as cell migration (Fig. 3*D*). Therefore, Wnt-5a could stimulate cell migration by regulating the activities of FAK and Rac, probably through PKC and Src.

The migration of MKN-1 cells in scratch-wound cultures was suppressed by knockdown of Wnt-5a (Fig. 4*A*). Ruffling and

phalloidin staining were observed at the cell front along the leading edge of control migrating cells (Fig. 4*B*). Paxillin is a focal adhesion protein (35). When the control MKN-1 cells were stained with anti-paxillin antibody, focal adhesions, including paxillin, were detected faintly (Fig. 4*B*). Knockdown of Wnt-5a obviously suppressed phalloidin staining at the leading edge, whereas it instead strengthened the formation of stress fibers and enlarged the size of focal adhesions, including paxillin (Fig. 4*B*). Because it has been suggested that the formation of large focal adhesions is due to the reduced turnover of adhesions (36), the effects of Wnt-5a on the dynamics of focal adhesions were examined. To this end, we expressed GFP-paxillin in MKN-1 cells and analyzed the turnover of dynamics by live fluorescence imaging. At the cell front in control cells, paxillin-containing adhesions disassembled as new adhesions were formed near the leading edge, whereas the turnover of paxillin-containing adhesions was suppressed in Wnt-5a knockdown cells (Fig. 4*C*). The rate constants of assembly and disassembly of GFP-paxillin at adhesion sites were decreased in Wnt-5a knockdown cells (Fig. 4*D*). These results suggest that Wnt-5a regulates the turnover of focal adhesion complexes, thereby stimulating cell migration.

Survival of gastric cancer patients with Wnt-5a expression. Finally, we examined the relationship between the expression of Wnt-5a and survival in advanced stages (T_2, T_3, and T_4) of gastric cancer (n = 111). The 5-year survival was 50% in patients with Wnt-5a-negative gastric cancer, whereas it was 20% in patients with Wnt-5a-positive gastric cancer (P < 0.0001; Fig. 5*A*, *a*). Furthermore, irrespective of histologic classification, the 5-year survival rate was significantly lower in patients with Wnt-5a-positive gastric cancer than in those with Wnt-5a-negative gastric cancer [P = 0.0036 for

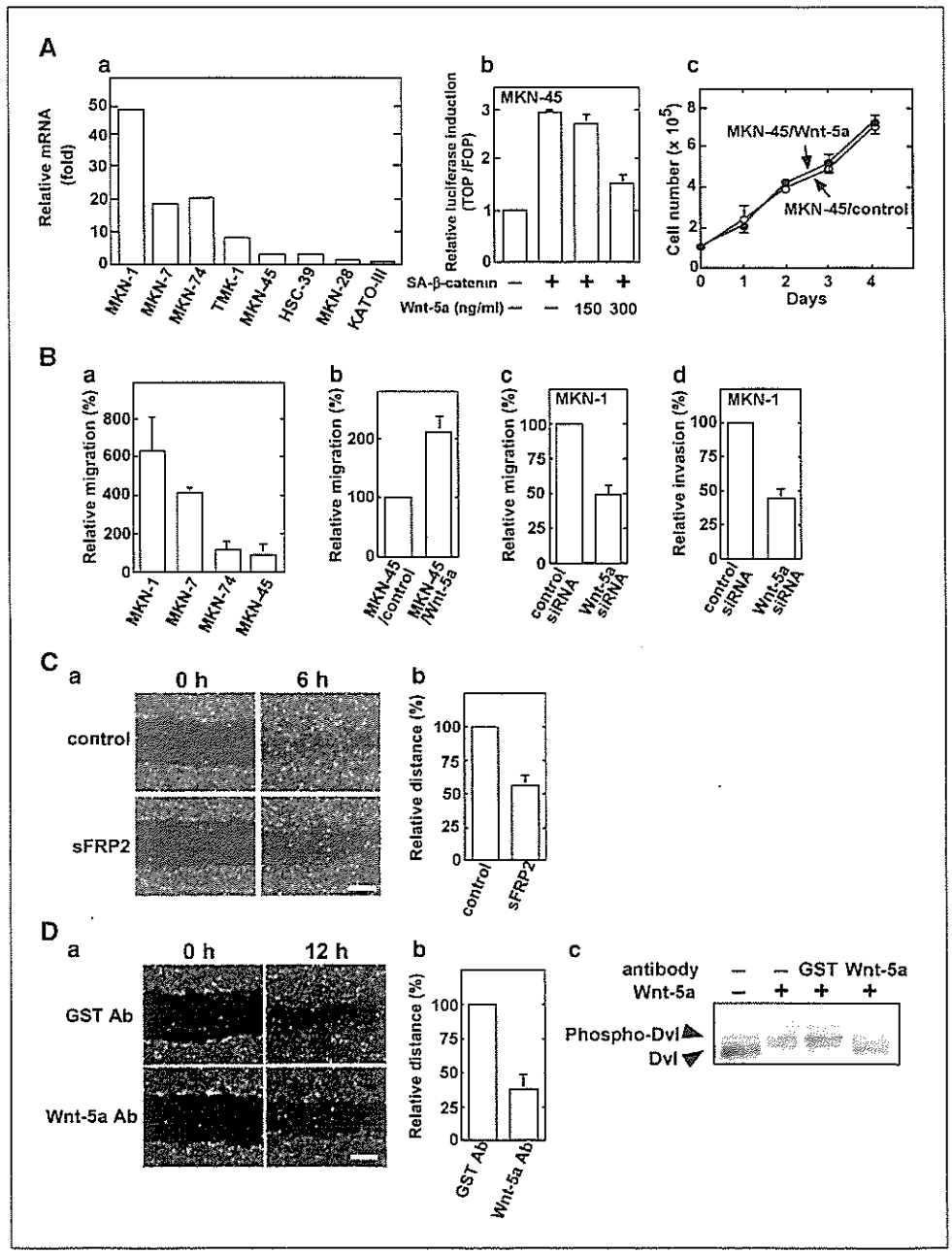

Figure 2. Actions of Wnt-5a on gastric cancer cells. *A*, inhibition of the β-catenin pathway by Wnt-5a. *a*, the level of expression of Wnt-5a mRNA in the gastric cancer cells was quantified by quantitative RT-PCR. *b*, after MKN-45 cells were transfected with pEF-BOS/hTcf-4E (0.1 μg), pUC/EF-1α/β-catenin^{SA} (0.5 μg), and TOP-*fos*-Luc (0.5 μg) or FOP-*fos*-Luc (0.5 μg), the cells were incubated with the indicated amounts of Wnt-5a for 8 hours. The luciferase activity was measured and expressed as the ratio of the activity in the cells transfected with TOP-*fos*-Luc to that in the cells transfected with FOP-*fos*-Luc. *c*, MKN-45 cells containing empty vector (MKN-45/control cells) or stably expressing Wnt-5a (MKN-45/Wnt-5a cells) were cultured in the presence of 2% serum for the indicated number of days, and then cell numbers were counted. *B*, stimulation of cell migration by Wnt-5a. *a*, the indicated gastric cells were placed in Transwell chamber for the migration assay. *b*, MKN-45/control cells or MKN-45/Wnt-5a cells were placed in Transwell chambers for the migration assay. *c* and *d*, MKN-1 cells transfected with the control or Wnt-5a siRNA were placed in noncoated (*c*) or Matrigel-coated (*d*) Transwell chambers for the migration or invasion assay, respectively. *C*, inhibition of cell migration by sFRP2. *a*, control or sFRP2 conditioned medium was added to MKN-1 cells, and then the cells were wounded. The culture was continued for 6 hours. Bar, 200 μm. *b*, migrating distances in (*a*) were measured. *D*, inhibition of cell migration by anti-Wnt-5a. *a*, MKN-1 cells incubated with anti-GST (as control) or anti-Wnt-5a antibody (50 μg/mL) were wounded. The culture was continued for 12 hours. Bar, 200 μm. *b*, migrating distances in (*a*) were measured. *Columns*, mean of three independent experiments; *bars*, SE. *c*, after Wnt-5a had been preincubated with anti-GST or anti-Wnt-5a antibody for 1 hour at 4°C, NIH3T3 cells were treated with 80 ng/mL Wnt-5a for 1 hour, and then cells were lysed and probed with anti-Dvl antibody.

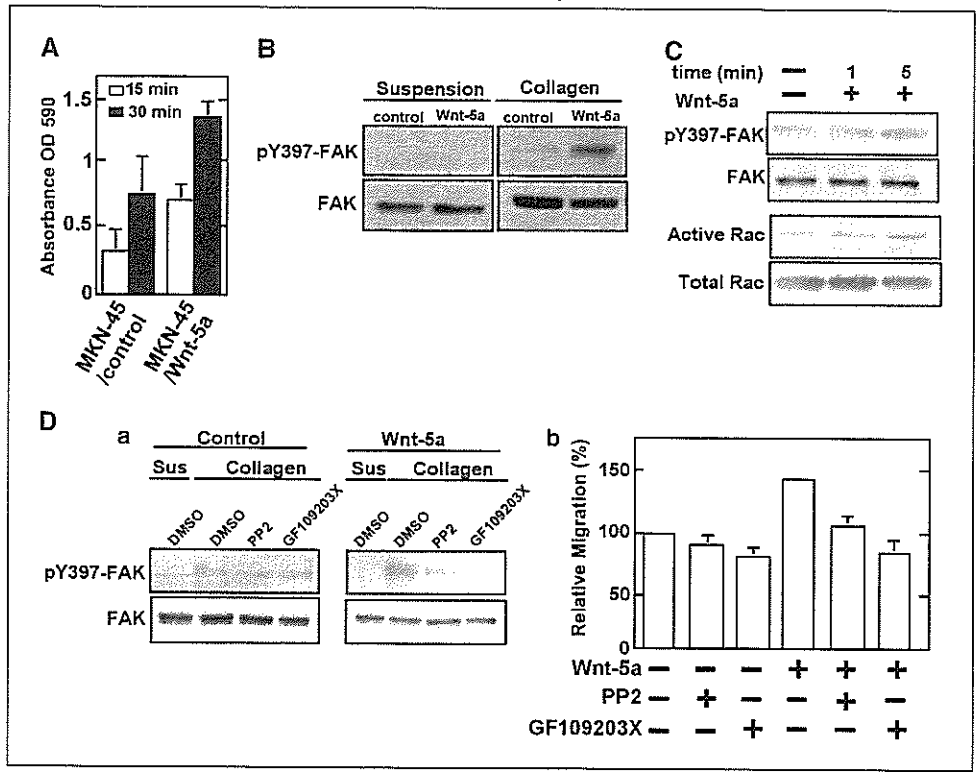

Figure 3. Molecular mechanism by which Wnt-5a stimulates cell migration. *A*, enhancement of cell adhesion by Wnt-5a. MKN-45/control or MKN-45/Wnt-5a cells were subjected to the adhesion assay for the indicated time. *B*, enhancement of collagen-induced activation of FAK by Wnt-5a. MNK-45/control and MKN-45/Wnt-5a cells were suspended in serum-free medium and kept in suspension or replated onto collagen-coated dishes. After 1 hour, the cells were lysed and probed with a phosphorylated specific antibody to FAK pTyr^{397} (*pY397-FAK*) or with anti-FAK antibody. *C*, activation of FAK and Rac by Wnt-5a. MKN-45 cells were treated with 80 ng/mL Wnt-5a for the indicated time, and then cells were lysed and probed with anti-pY397-FAK or anti-FAK antibody. The same lysates were incubated with GST-CRIB immobilized on glutathione-Sepharose. The total lysates and precipitates were probed with anti-Rac-1 antibody. *D*, involvement of PKC and Src in Wnt-5a-induced activation of FAK and cell migration. *a*, after MKN-45/control and MKN-45/Wnt-5a cells were treated with 62.5 nmol/L PP2 or GF109203X for 60 minutes, the cells were suspended in serum-free medium and kept in suspension (*Sus*) or replated onto collagen-coated dish. After 1 hour, the cells were lysed and probed with anti-pY397-FAK or anti-FAK antibody. *b*, after MKN-45 cells were treated with 62.5 nmol/L PP2 or GF109203X, the cells were subjected to the Transwell migration assay in the presence or absence of 600 ng/mL Wnt-5a.

diffuse-scattered type (n = 40); P = 0.0014 for other type (n = 71); Fig. 5*A*, *b* and *c*].

It has been reported that the expression of MIA, EGFR, or MMP-10 is associated with the aggressiveness of tumors, including gastric cancer (37). Although the prognosis of patients expressing MIA, EGFR, or MMP-10 was significantly worse (P < 0.0001, P = 0.0049, and P = 0.0122, respectively), the prognostic value of MIA was comparable with that of Wnt-5a (Fig. 5*B*, *a-c*). Cytosomal and nuclear accumulation of β-catenin did not show a significant association with the survival of gastric cancer (P = 0.4873; Fig. 5*B*, *d*).

It is generally known that patients with gastric cancer at stage I and stage IV show a good and poor survival, respectively, but it is difficult to predict the prognosis of patients with gastric cancer at stage II and stage III. Therefore, we analyzed the prognostic value of Wnt-5a, MIA, EGFR, or MMP-10 in the group of patient with gastric cancer at stage II and stage III (n = 56). The patients with Wnt-5a-positive gastric cancer had a significantly worse rate of survival than the patients with Wnt-5a-negative gastric cancer (P = 0.0137; Fig. 5*C*, *a*). In contrast, there was no significant association between the expression of MIA, EGFR, or MMP-10 and the survival of patients with gastric cancer at stages II and stage III (data not shown). The patients with gastric cancer at stage III indeed had the shorter survival time than those at stage II (P = 0.0431; Fig. 5*C*, *b*). These results clearly indicate that the 5-year survival of gastric cancer is associated with expression of Wnt-5a in a histology-independent manner and suggest that Wnt-5a is a good prognostic indicator for gastric cancer patients.

Discussion

Gastric cancer is one of the leading causes of death due to cancer worldwide (21, 38). In this study, we showed that Wnt-5a is required for the migration and invasive ability of gastric cancer cells and that the expression of Wnt-5a is correlated with aggressiveness and poor prognosis of gastric cancer. It is notable that prognosis is not dependent on histologic type but rather is dependent on expression of Wnt-5a. Wnt-5a positivity is correlated with a poor prognosis of gastric cancer patients with stage II or stage III despite lack of statistical significance of other prognostic markers. Because it is hard to predict the prognosis of these patients, investigating the staining of Wnt-5a in gastric cancer cells may be helpful for determining the therapeutic strategy after surgical operation. Considering the results that sFRP2, anti-Wnt-5a antibody, or siRNA for Wnt-5a inhibits the cell migration of gastric cancer cells, Wnt-5a is not only a good prognostic indicator of gastric cancer but also a candidate for a molecular target of therapy for gastric cancer.

We also found that Wnt-5a is expressed in Chief cells in normal gastric mucosa. It is generally believed that stem cells are present

in the proliferative cell zone in the isthmus region of the gastric glands and that cells derived from stem cells undergo complex bipolar migration from the isthmus either upward or downward. Wnt-5a may be involved in the downward migration of cells differentiating into normal Chief cells.

Wnt-5a has been reported to be capable of activating JNK, which regulates convergent extension movement in *Xenopus* embryos and stimulates invasion of breast cancer cells (20, 39). However, the molecular mechanism by which Wnt-5a regulates cell migration is not fully understood. Cell migration is a complex cellular behavior that involves protrusion and adhesion at the cell front and contraction and detachment at the rear (36). FAK activation is best understood in the context of the engagement of integrins at the cell surface (34). Activation of FAK results in recruitment of several SH2 domain– and SH3 domain–containing proteins. Among them, p130Cas and Crk are involved in cell migration. Small G protein Rac also plays an important role in cell migration by regulating adhesion turnover and the lamellipodium (40). Dominant-negative Rac blocks the increased migration in response to the expression of p130Cas and Crk, probably through DOCK180, which suggests that Rac acts as a downstream effector of the FAK-Cas-Crk complex.

We showed that Wnt-5a is involved in the activation of FAK and Rac, the turnover of paxillin, and the membrane ruffling. Inhibitors of PKC and Src suppressed Wnt-5a-dependent cell migration and FAK activation. It has been shown that Wnt-5a activates PKC (3) and that JNK-dependent phosphorylation of paxillin and PKC-dependent activation of FAK are important for cell migration (34, 41). These findings suggest that Wnt-5a activates PKC and JNK, thereby leading to the activation of FAK and paxillin. Taken together, these results make it conceivable that Wnt-5a and

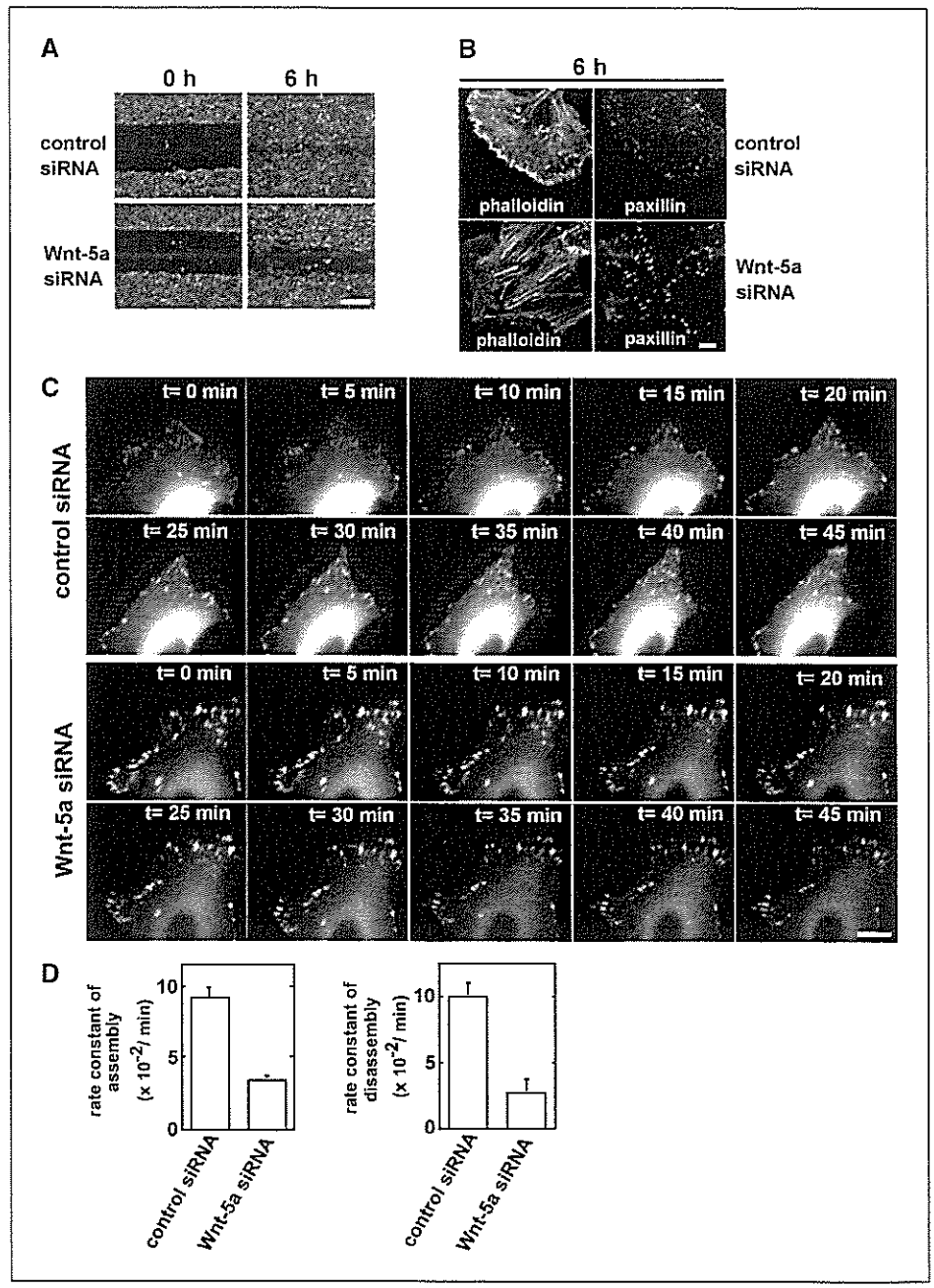

Figure 4. Effects of Wnt-5a on dynamics of focal adhesions. *A*, MKN-1 cells transfected with the control or Wnt-5a siRNA for 6 hours were wounded. Bar, 200 μm. *B*, MKN-1 cells transfected with the control or Wnt-5a siRNA were stained with FITC-labeled phalloidin for visualization of F-actin at 6 hours after wounding. The same cells were stained with anti-paxillin antibody. Bar, 10 μm. *C*, dynamics of GFP-paxillin in MKN-1 cells treated with the control or Wnt-5a siRNA visualized by time-lapse fluorescence microscopy. Bar, 5 μm. *D*, rate constants of assembly and disassembly of GFP-paxillin in (*C*) were calculated.

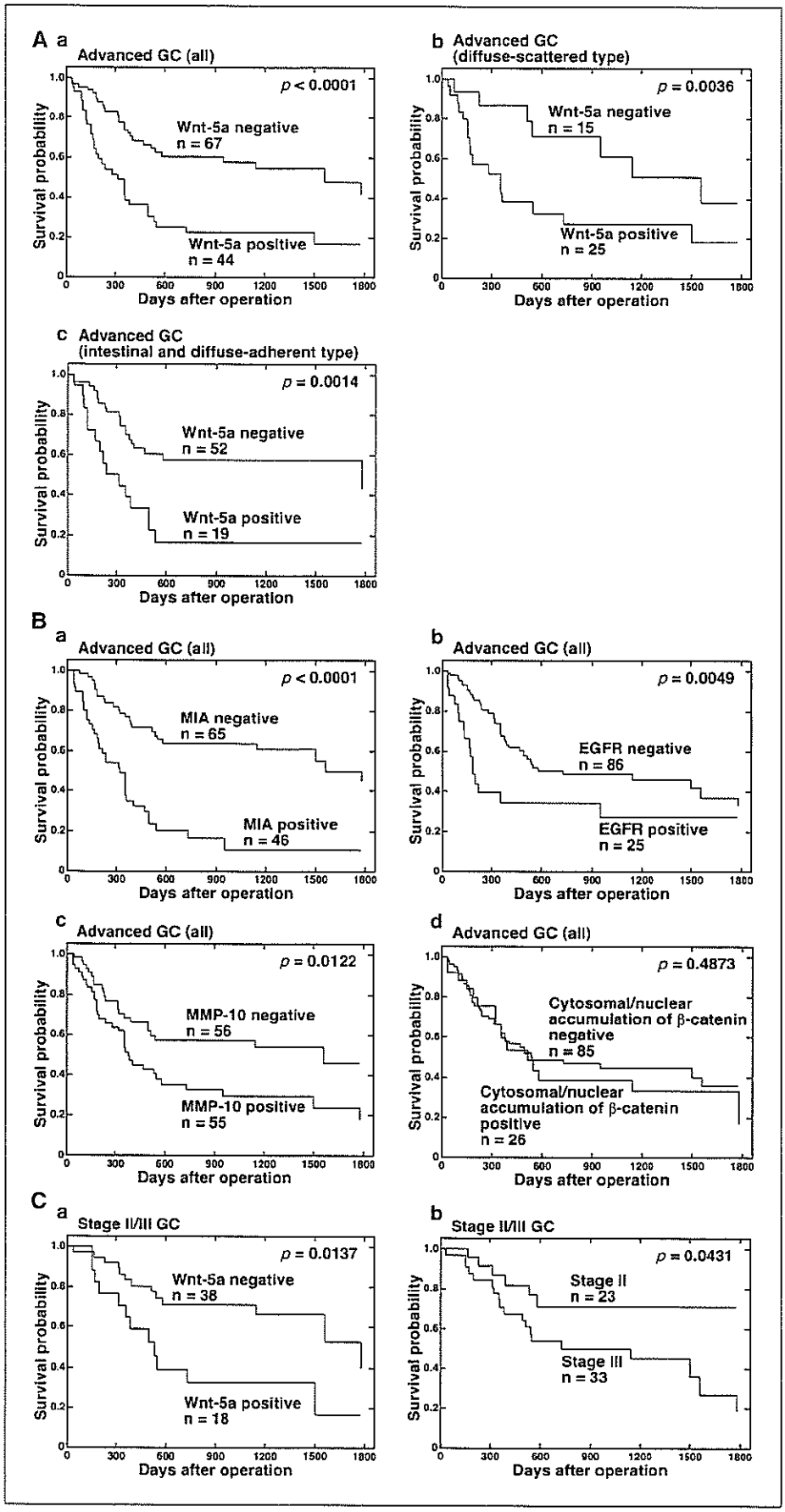

Figure 5. Overall survival of gastric cancer patients with Wnt-5a expression. *A*, association of expression of Wnt-5a with poor prognosis irrespective histologic type. *a*, all advanced stages of gastric cancer patients (n = 111); *b*, diffuse-scattered-type gastric cancer patients (n = 40); *c*, other type gastric cancer patients (n = 71). *B*, comparison with other prognostic factors. *a*, gastric cancer patients with or without MIA expression (n = 111); *b*, gastric cancer patients with or without EGFR expression (n = 111); *c*, gastric cancer patients with or without MMP-10 expression (n = 111); *d*, gastric cancer patients with or without β-catenin expression in cytoplasm and nucleus (n = 111). *C*, expression of Wnt-5a in stages II and III gastric cancer. *a*, stage II and III gastric cancer patients with or without Wnt-5a expression (n = 56); *b*, survival of stage II and III gastric cancer patients (n = 56).

extracellular matrix bind to Frizzled (Wnt-5a receptor) and integrin and cooperatively activate a signaling cascade to stimulate cell migration. Therefore, it is conceivable that overexpression of Wnt-5a acts as a migration activator in gastric cancer.

In addition, Wnt-5a has been suggested to act as a tumor suppressor in lymphoma, thyroid cancer, and colon cancer (15–17) because Wnt-5a inhibits the β-catenin pathway (12, 13). Our result indicated that Wnt-5a neither induces the accumulation of β-catenin nor inhibits Wnt-3a-dependent-accumulation of β-catenin in HEK293 and NIH3T3 cells (data not shown). Although Topol et al. (11) showed that Wnt-5a induces the down-regulation of β-catenin through expression of Siah2, we could not repeat this finding and our results were rather consistent with those showed by Mikels and Nusse (13). Whereas Topol et al. transfected Wnt-5a cDNA in HEK293 or SW480 cells, we added purified Wnt-5a protein to HEK293 and NIH3T3 cells. Although the reasons for the discrepancy between their and our results are not known at present, one possibility might be due to different assay conditions. Instead, we showed that Wnt-5a inhibits β-catenin-dependent Tcf activation downstream of β-catenin. It has been shown that transforming growth factor-β–activated kinase (TAK) and Nemo-like kinase (NLK) mediate Wnt-5a-dependent suppression of Tcf activity (12), but dominant negative forms of TAK or NLK did not influence it in our hands (data not shown). Therefore, the mechanism for the inhibition of the β-catenin pathway by Wnt-5a is not clear.

Among 237 gastric cancer cases, gastric cancer abnormally expressing both Wnt-5a and β-catenin were observed in only one gastric cancer case, suggesting that the expression of Wnt-5a and β-catenin is mutually exclusive. As Wnt-5a acts as a negative regulator for β-catenin-dependent cellular proliferation, the β-catenin-positive cells may prevent the expression of Wnt-5a. Although the exact mechanism for the exclusive expression of Wnt-5a and β-catenin in gastric cancer is not known, there may be some mechanisms by which the β-catenin signaling and the Wnt-5a signaling mutually suppress the expression of Wnt-5a and β-catenin. Genetic alterations that cause abnormal expression of β-catenin in cancer cells are well understood, but how expression of Wnt-5a is regulated is totally unknown. It seems unlikely that *Wnt-5a* gene is amplified or rearranged in prostate cancer or melanoma (18). It has also been reported that expression of Wnt-5a mRNA is suppressed by Ras and hepatocyte growth factor (HGF; refs. 42, 43). It is intriguing to speculate that β-catenin mediates Ras- or HGF-induced suppression of Wnt-5a. Furthermore, whether mutually exclusive expression of Wnt-5a and β-catenin is specific for gastric cancer or not remains to be clarified. Therefore, immunohistochemical analyses of β-catenin are necessary for investigation of Wnt-5a in human cancers. Further studies will be necessary to understand the functions of Wnt-5a and the pathologic significance of the abnormal expression of Wnt-5a in cancer cells.

Acknowledgments

Received 6/28/2006; revised 8/14/2006; accepted 8/31/2006.

Grant support: Grants-in-Aid for Scientific Research and for Scientific Research on Priority Areas from the Ministry of Education, Science, and Culture, Japan (2004, 2005, and 2006).

The costs of publication of this article were defrayed in part by the payment of page charges. This article must therefore be hereby marked *advertisement* in accordance with 18 U.S.C. Section 1734 solely to indicate this fact.

We thank Drs. H. Clevers, A. Nagafuchi, T. Akiyama, H. Sabe, and K. Kaibuchi for donating plasmids.

References

1. Wodarz A, Nusse R. Mechanisms of Wnt signaling in development. Annu Rev Cell Dev Biol 1998;14:59–88.
2. Wong GT, Gavin BJ, McMahon AP. Differential transformation of mammary epithelial cells by wnt genes. Mol Cell Biol 1994;14:6278–86.
3. Kuhl M, Sheldahl LC, Park M, Miller JR, Moon RT. The Wnt/Ca2$^+$ pathway: a new vertebrate wnt signaling pathway takes shape. Trends Genet 2000;16:279–83.
4. Ikeda S, Kishida S, Yamamoto H, Murai H, Koyama S, Kikuchi A. Axin, a negative regulator of the Wnt signaling pathway, forms a complex with GSK-3b and b-catenin and promotes GSK-3b-dependent phosphorylation of b-catenin. EMBO J 1998;17:1371–84.
5. Kitagawa M, Hatakeyama S, Shirane M, et al. An F-box protein, FWD1, mediates ubiquitin-dependent proteolysis of b-catenin. EMBO J 1999;18:2401–10.
6. Kikuchi A. Roles of Axin in the Wnt signalling pathway. Cell Signal 1999;11:777–88.
7. Liu C, Li Y, Semenov M, et al. Control of b-catenin phosphorylation/degradation by a dual-kinase mechanism. Cell 2002;108:837–47.
8. He X, Semenov M, Tamai K, Zeng X. LDL receptor-related proteins 5 and 6 in Wnt/b-catenin signaling: arrows point the way. Development 2004;131:1663–77.
9. Hurlstone A, Clevers H. T-cell factors: turn-ons and turn-offs. EMBO J 2002;21:2303–11.
10. Kohn AD, Moon RT. Wnt and calcium signaling: b-catenin-independent pathways. Cell Calcium 2005;38:439–336.
11. Topol L, Jiang X, Choi H, Garrett-Beal L, Carolan PJ, Yang Y. Wnt-5a inhibits the canonical Wnt pathway by promoting GSK-3-independent b-catenin degradation. J Cell Biol 2003;162:899–908.
12. Ishitani T, Kishida S, Hyodo-Miura J, et al. The TAK1-NLK mitogen-activated protein kinase cascade functions in the Wnt-5a/Ca2$^+$ pathway to antagonize Wnt/b-catenin signaling. Mol Cell Biol 2003;23:131–9.
13. Mikels AJ, Nusse R. Purified Wnt5a protein activates or inhibits b-catenin-TCF signaling depending on receptor context. PLoS Biol 2006;4:570–82.
14. Olson DJ, Gibo DM. Antisense wnt-5a mimics wnt-1-mediated C57MG mammary epithelial cell transformation. Exp Cell Res 1998;241:134–41.
15. Liang H, Chen Q, Coles AH, et al. Wnt5a inhibits B cell proliferation and functions as a tumor suppressor in hematopoietic tissue. Cancer Cell 2003;4:349–60.
16. Kremenevskaja N, von Wasielewski R, Rao AS, Schofl C, Andersson T, Brabant G. Wnt-5a has tumor suppressor activity in thyroid carcinoma. Oncogene 2005;24:2144–54.
17. Dejmek J, Dejmek A, Safholm A, Sjolander A, Andersson T. Wnt-5a protein expression in primary dukes B colon cancers identifies a subgroup of patients with good prognosis. Cancer Res 2005;65:9142–6.
18. Iozzo RV, Eichstetter I, Danielson KG. Aberrant expression of the growth factor Wnt-5A in human malignancy. Cancer Res 1995;55:3495–9.
19. Weeraratna AT, Jiang Y, Hostetter G, et al. Wnt5a signaling directly affects cell motility and invasion of metastatic melanoma. Cancer Cell 2002;1:279–88.
20. Pukrop T, Klemm F, Hagemann T, et al. Wnt 5a signaling is critical for macrophage-induced invasion of breast cancer cell lines. Proc Natl Acad Sci U S A 2006;103:5454–9.
21. Ohgaki H, Matsukura N. Stomach cancer. Lyon: IARC Press; 2003. p. 197.
22. Kishida S, Yamamoto H, Kikuchi A. Wnt-3a and Dvl induce neurite retraction by activating Rho-associated kinase. Mol Cell Biol 2004;24:4487–501.
23. Lauren P. The two histological main types of gastric carcinoma: diffuse and so-called intestinal-type carcinoma. An attempt at a histo-clinical classification. Acta Pathol Microbiol Scand 1965;64:31–49.
24. Oue N, Motoshita J, Yokozaki H, et al. Distinct promoter hypermethylation of p16INK4a, CDH1, and RAR-β in intestinal, diffuse-adherent, and diffuse-scattered type gastric carcinomas. J Pathol 2002;198:55–9.
25. Aung PP, Oue N, Mitani Y, et al. Systematic search for gastric cancer-specific genes based on SAGE data: melanoma inhibitory activity and matrix metalloproteinase-10 are novel prognostic factors in patients with gastric cancer. Oncogene 2006;25:2546–57.
26. Yamamoto H, Ihara M, Matsuura Y, Kikuchi A. Sumoylation is involved in b-catenin-dependent activation of Tcf-4. EMBO J 2003;22:2047–59.
27. Kobayashi T, Hino S, Oue N, et al. Glycogen synthase kinase 3 and h-prune regulate cell migration by modulating focal adhesions. Mol Cell Biol 2006;26:898–911.
28. Hino S, Tanji C, Nakayama K-I, Kikuchi A. Phosphorylation of b-catenin by cyclic AMP-dependent protein kinase stabilizes b-catenin through inhibition of its ubiquitination. Mol Cell Biol 2005;25:9063–72.
29. Ihara M, Yamamoto H, Kikuchi A. SUMO-1 modification of PIASy, an E3 ligase, is necessary for PIASy-dependent activation of Tcf-4. Mol Cell Biol 2005;25:3506–18.
30. Zheng L, Wang L, Ajani J, Xie K. Molecular basis of gastric cancer development and progression. Gastric Cancer 2004;7:61–77.
31. Yokozaki H. Molecular characteristics of eight gastric cancer cell lines established in Japan. Pathol Int 2000;50:767–77.
32. Kawano Y, Kypta R. Secreted antagonists of the Wnt signalling pathway. J Cell Sci 2003;116:2627–34.
33. Gonzalez-Sancho JM, Brennan KR, Castelo-Soccio LA, Brown AM. Wnt proteins induce dishevelled

phosphorylation via an LRP5/6- independent mechanism, irrespective of their ability to stabilize b-catenin. Mol Cell Biol 2004;24:4757–68.
34. Parsons JT. Focal adhesion kinase: the first ten years. J Cell Sci 2003;116:1409–16.
35. Turner CE. Paxillin and focal adhesion signalling. Nat Cell Biol 2000;2:E231–6.
36. Ridley AJ, Schwartz MA, Burridge K, et al. Cell migration: integrating signals from front to back. Science 2003;302:1704–9.
37. Yasui W, Oue N, Aung PP, Matsumura S, Shutoh M, Nakayama H. Molecular-pathological prognostic factors of gastric cancer. Gastric Cancer 2005;8:86–94.
38. Ushijima T, Sasako M. Focus on gastric cancer. Cancer Cell 2004;5:121–5.
39. Yamanaka H, Moriguchi T, Masuyama N, et al. JNK functions in the non-canonical Wnt pathway to regulate convergent extension movements in vertebrates. EMBO Rep 2002;3:69–75.
40. Etienne-Manneville S, Hall A. Rho GTPases in cell biology. Nature 2002;420:629–35.
41. Huang C, Rajfur Z, Borchers C, Schaller MD, Jacobson K. JNK phosphorylates paxillin and regulates cell migration. Nature 2003;424:219–23.
42. Huguet EL, Smith K, Bicknell R, Harris AL. Regulation of Wnt5a mRNA expression in human mammary epithelial cells by cell shape, confluence, and hepatocyte growth factor. J Biol Chem 1995;270:12851–6.
43. Bui TD, Tortora G, Ciardiello F, Harris AL. Expression of Wnt5a is downregulated by extracellular matrix and mutated c-Ha-ras in the human mammary epithelial cell line MCF-10A. Biochem Biophys Res Commun 1997;239:911–7.

The Neuromedin U-Growth Hormone Secretagogue Receptor 1b/Neurotensin Receptor 1 Oncogenic Signaling Pathway as a Therapeutic Target for Lung Cancer

Koji Takahashi,[1] Chiyuki Furukawa,[1,4] Atsushi Takano,[1] Nobuhisa Ishikawa,[1] Tatsuya Kato,[1] Satoshi Hayama,[1] Chie Suzuki,[1] Wataru Yasui,[2] Kouki Inai,[3] Saburo Sone,[4] Tomoo Ito,[5] Hitoshi Nishimura,[6] Eiju Tsuchiya,[7] Yusuke Nakamura,[1] and Yataro Daigo[1]

[1]Laboratory of Molecular Medicine, Human Genome Center, Institute of Medical Science, The University of Tokyo, Tokyo, Japan; Departments of [2]Molecular Pathology and [3]Pathology, Graduate School of Biomedical Sciences, Hiroshima University, Hiroshima, Japan; [4]Department of Internal Medicine and Molecular Therapeutics, The University of Tokushima School of Medicine, Tokushima, Japan; [5]Department of Surgical Pathology, Hokkaido University Graduate School of Medicine, Sapporo, Japan; [6]Department of Thoracic Surgery, Saitama Cancer Center, Saitama, Japan; and [7]Kanagawa Cancer Center Research Institute, Kanagawa, Japan

Abstract

Using a genome-wide cDNA microarray to search for genes that were specifically up-regulated in non–small cell lung cancers (NSCLC), we identified an abundant expression of neuromedin U (NMU) in the great majority of lung cancers. Immunohistochemical analysis showed a significant association of NMU expression with poorer prognosis of patients with NSCLC. Treatment of NSCLC cells with short interfering RNA against NMU suppressed its expression and inhibited the growth of the cells; on the other hand, the induction of exogenous expression of NMU conferred growth-promoting activity and enhanced cell mobility *in vitro*. We found that two G protein–coupled receptors, growth hormone secretagogue receptor 1b and neurotensin receptor 1, were also overexpressed in NSCLC cells, and that a heterodimer complex of these receptors functioned as an NMU receptor. The NMU-receptor interaction subsequently induced the generation of a second messenger, cyclic AMP, to activate its downstream genes including transcription factors and cell cycle regulators. Treatment of NSCLC cells with short interfering RNAs for growth hormone secretagogue receptor or neurotensin receptor 1 suppressed the expression of those genes and the growth of NSCLC cells. These data strongly implied that targeting the NMU signaling pathway would be a promising therapeutic strategy for the treatment of lung cancers. (Cancer Res 2006; 66(19): 9408-19)

Introduction

Lung cancer is one of the most common causes of cancer death worldwide, and non–small cell lung cancer (NSCLC) accounts for nearly 80% of those cases (1). Many genetic alterations associated with the development and progression of lung cancer have been reported, but the precise molecular mechanisms remain unclear (2). Over the last decade, newly developed cytotoxic agents including paclitaxel, docetaxel, gemcitabine, and vinorelbine have emerged to offer multiple therapeutic choices for patients with advanced NSCLC; however, each of the new regimens can provide only modest survival benefits compared with cisplatin-based therapies (3). Hence, new therapeutic strategies, such as the development of molecular-targeted agents, are eagerly awaited.

Systematic analysis of expression levels of thousands of genes on cDNA microarrays is an effective approach to identifying unknown molecules involved in pathways of carcinogenesis (4–11), and can reveal candidate targets for the development of novel anticancer drugs and tumor markers. We have been attempting to isolate novel molecular targets for the diagnosis, treatment, and prevention of NSCLC by analyzing genome-wide expression profiles of NSCLC cells on a cDNA microarray containing 23,040 genes, after pure populations of tumor cells were prepared from 37 cancer tissues by laser microdissection (4). To verify the biological and clinicopathologic significance of the respective gene products, we have been performing tumor-tissue microarray analysis of clinical lung cancer materials (7–9, 11). In the course of those studies, we observed that the gene encoding neuromedin U (NMU) was frequently overexpressed in primary NSCLCs.

NMU is a neuropeptide that was first isolated from porcine spinal cord. It has potent activity on smooth muscle (12–17), and in mammalian species, NMU is distributed predominantly in the gastrointestinal tract and central nervous system (18, 19). The peripheral activities of NMU include stimulation of smooth muscle, alternation of ion transport in the gut, and regulation of feeding (12); however, any role which NMU might have during lung carcinogenesis has not been implicated. Neuropeptides function peripherally as paracrine and autocrine factors to regulate diverse physiologic processes and act as neurotransmitters or neuromodulators in the nervous system. In general, the receptors which mediate signaling by binding neuropeptides are members of the superfamily of G protein–coupled receptors (GPCR) having seven transmembrane-spanning domains. Two known receptors for NMU, NMU1R and NMU2R, show a high degree of homology to other neuropeptide receptors such as growth hormone secretagogue receptor (GHSR) and neurotensin receptor 1 (NTSR1), for which the corresponding known ligands are ghrelin (GHRL) and neurotensin (NTS), respectively.

In the study reported here, we identified NMU and its downstream molecules as potential targets for the development of novel therapeutic drugs and diagnostic markers. We also show that GHSR1b and NTSR1 could be a cognate heterodimerized receptor complex for NMU, and that this ligand-receptor system significantly affects the growth of lung cancer cells through the

Note: Supplementary data for this article are available at Cancer Research Online (http://cancerres.aacrjournals.org/).

K. Takahashi and C. Furukawa contributed equally to this work.

Requests for reprints: Yataro Daigo, Laboratory of Molecular Medicine, Human Genome Center, Institute of Medical Science, The University of Tokyo, Tokyo 108-8639, Japan. Phone: 81-3-5449-5457; Fax: 81-3-5449-5406; E-mail: ydaigo@ims.u-tokyo.ac.jp.

doi:10.1158/0008-5472.CAN-06-1349

transactivation of its downstream signals involving transcription factors and cell cycle regulators.

Materials and Methods

Cell lines and clinical tissue samples. The 19 human lung cancer cell lines used in this study were as follows: 15 NSCLCs—A549, NCI-H23, NCI-H358, NCI-H522, NCI-H1435, NCI-H1793, LC174, LC176, LC319, PC3, PC9, PC14, SK-LU-1, RERF-LC-AI, and SK-MES-1; and 4 small cell lung cancers (SCLC)—SBC-3, SBC-5, DMS114, and DMS273. All cells were grown in the appropriate medium supplemented with 10% FCS and were maintained at 37°C in an atmosphere of humidified air with 5% CO_2.

Primary NSCLC samples had been obtained earlier with informed consent from 37 patients (4). Fifteen additional primary NSCLCs, including seven adenocarcinomas and eight squamous cell carcinomas, were obtained along with adjacent normal lung tissue samples from patients undergoing surgery at Hokkaido University and its affiliated hospitals (Sapporo, Japan).

A total of 326 formalin-fixed primary NSCLCs (stage I-IIIa) including 224 adenocarcinomas, 86 squamous cell carcinomas, 13 large-cell carcinomas, and 3 adenosquamous carcinomas, and adjacent normal lung tissue samples were obtained from patients who underwent surgery at Hokkaido University and its affiliated hospitals (Sapporo, Japan), and Saitama Cancer Center (Saitama, Japan). Large cell neuroendocrine carcinoma samples from three patients were obtained from the Saitama Cancer Center. Samples of advanced SCLC (stage IV) from postmortem materials (17 individuals) obtained from Hiroshima University (Hiroshima, Japan), were also used in this study. The use of all clinical materials was approved by the Institutional Research Ethics Committees.

Semiquantitative reverse transcription-PCR analysis. Total RNA was extracted from cultured cells and clinical tissues using Trizol reagent (Life Technologies, Inc., Gaithersburg, MD) according to the manufacturer's protocol. Extracted RNAs and normal human tissue polyadenylate RNAs were treated with DNase I (Nippon Gene, Tokyo, Japan) and were reverse-transcribed using oligo$(dT)_{20}$ primer and SuperScript II reverse transcriptase (Invitrogen, Carlsbad, CA). Semiquantitative reverse transcription-PCR (RT-PCR) experiments were carried out with the following synthesized gene-specific primers or with β-actin (*ACTB*)-specific primers as an internal control: *NMU*, 5′-TGAAGAGATTCAGAGTGGACGA-3′ and 5′-ACTGAGAACATTGACAACACAGG-3′; *NMU1R*, 5′-AAGAGGGACAGGGACAAGTAGT-3′ and 5′-ATGCCACTGTTACTGCTTCAG-3′; *NMU2R*, 5′-GGCTCTTACAACTCATGTACCCA-3′ and 5′-TGATACAGAGACATGAAGTGAGCA-3′; *GHSR1a*, 5′-TGGTGTTTGCCTTCATCCT-3′ and 5′-GAATCCCAGAAGTCTGAACA-3′; *GHSR1b*, 5′-CTTGGGACACCAACGAGTG-3′ and 5′-AGGACCCGCGAGAGAAAGC-3′; *NTSR1*, 5′-GGTCTGTGGCTGTGACTGAA-3′ and 5′-GTTTGAGCTGTGAGGGCTGT-3′; *GHRL*, 5′-TGAGCCCTGAACACCAGAGAG-3′ and 5′-AAAGCCAGATGAGCGCTTCTA-3′; *NTS*, 5′-TCTTCAGCATGATGTGTTGTGT-3′ and 5′-TGAGAGATTCATGAGGAAGTCTTG-3′; *FOXM1*, 5′-CCCTGACAACATCAACTGGTC-3′ and 5′-GTCCACCTTCGCTTTTATTGAGT-3′; unannotated transcript (clone IMAGE:3839141, mRNA), 5′-AAAAAGGGGATGCCTAGAACTC-3′ and 5′-CTTTCAGCACGTCAAGGACAT-3′; *GCDH*, 5′-ACACCTACGAAGGTACACATGAC-3′ and 5′-GCTATTTCAGGGTAAATGGAGTC-3′; *CDK5RAP1*, 5′-CAGAGATGGAGGATGTCAATAAC-3′ and 5′-CATAGCAGCTTTAAAGAGACACG-3′; *LOC134145*, 5′-CCACCATAACAGTGGAGTGGG-3′ and 5′-CAGTTACAGGTGTATGACTGGGAG-3′; *NUP188*, 5′-CTGAATACAACTTCCTGTTTGCC-3′ and 5′-GACCACAGAATTACCAAAACTGC-3′; *ACTB*, 5′-GAGGTGATAGCATTGCTTTCG-3′ and 5′-CAAGTCAGTGTACAGGTAAGC-3′. PCR reactions were optimized for the number of cycles to ensure product intensity within the logarithmic phase of amplification.

Northern blot analysis. Human multiple-tissue blots (BD Biosciences Clontech, Palo Alto, CA) were hybridized with a ^{32}P-labeled PCR product of *NMU*. The full-length cDNA of *NMU* was prepared by RT-PCR using primers 5′-CGCGGATCCGCGATGCTGCGAACAGAGAGCTG-3′ and 5′-CCGCTCGAGCGGAATGAACCCTGCTGACCTTC-3′. Prehybridization, hybridization, and washing were done according to the supplier's recommendations. The blots were autoradiographed with intensifying screens at room temperature for 72 hours.

Western blotting. Cells were lysed with radioimmunoprecipitation assay buffer [50 mmol/L Tris-HCl (pH 8.0), 150 mmol/L NaCl, 1% NP40, 0.5% deoxychorate-Na, 0.1% SDS] containing Protease Inhibitor Cocktail Set III (Calbiochem, Darmstadt, Germany). Protein samples were separated by SDS-polyacrylamide gels and electroblotted onto Hybond-ECL nitrocellulose membranes (GE Healthcare Bio-Sciences, Piscataway, NJ). Blots were incubated with a rabbit polyclonal anti-NMU antibody (generated to recombinant NMU), mouse monoclonal anti-FLAG M2 antibody (Sigma-Aldrich, Co., St. Louis, MO), goat polyclonal anti-NTSR1 antibody (Santa Cruz Biotechnology, Inc., Santa Cruz, CA), and rabbit polyclonal anti-GHSR antibody (generated to the peptide GVEHENGTDPWDTNEC). Antigen-antibody complexes were detected using secondary antibodies conjugated to horseradish peroxidase (GE Healthcare Bio-Sciences). Protein bands were visualized by enhanced chemiluminescence Western blotting detection reagents (GE Healthcare Bio-Sciences).

Immunohistochemistry and tissue microarray. To investigate the presence of NMU, GHSR1b, NTSR1, or FOXM1 protein in clinical samples (normal lung tissues, NSCLCs, and SCLCs that had been embedded in the paraffin block), we stained the sections using ENVISION+ Kit/horseradish peroxidase (DakoCytomation, Glostrup, Denmark). Briefly, each polyclonal antibody to NMU, GHSR1b (generated to the peptide GGSQRALRLSLAGPILSLC), NTSR1, or FOXM1 (Santa Cruz Biotechnology) was added after blocking endogenous peroxidase and proteins, and the sections were incubated with horseradish peroxidase–labeled anti-rabbit IgG and anti-goat IgG as the secondary antibody. Substrate chromogen was added and the specimens were counterstained with hematoxylin.

The tumor tissue microarrays were constructed as published previously (20, 21). The tissue area for sampling was selected based on a visual alignment with the corresponding H&E-stained section on a slide. Three-, four-, or five-tissue cores (diameter, 0.6 mm; height, 3-4 mm) taken from the donor tumor blocks were placed into a recipient paraffin block using a tissue microarrayer (Beecher Instruments, Sun Prairie, WI). A core of normal tissue was punched from each case. Five-micrometer sections of the resulting microarray block were used for immunohistochemical analysis. NMU positivity was assessed according to staining intensity as absent (no visible staining in tumor cells) or positive (dark brown staining in >50% of tumor cells completely obscuring cytoplasm) by three independent investigators without prior knowledge of the clinical follow-up data. The intensity of GHSR1b or NTSR1 staining was evaluated as well using the following criteria: positive, dark brown staining in >50% of tumor cells completely obscuring membrane and cytoplasm; absent, no appreciable staining in tumor cells. The intensity of FOXM1 staining was evaluated using the following criteria: positive, dark brown staining in >50% of tumor cells completely obscuring nucleus and cytoplasm; absent, no appreciable staining in tumor cells. Cases were accepted only as positive if reviewers independently defined them as such.

Statistical analysis. Tumor-specific survival curves were calculated from the date of surgery to the time of death related to NSCLC, or to the last follow-up observation. Kaplan-Meier curves were calculated for each relevant variable; differences in survival times among patient subgroups were analyzed using the log-rank test. Univariate and multivariate analyses were done using Cox's proportional hazard regression model to determine associations between clinicopathologic variables and cancer-related mortality. $P < 0.05$ were considered statistically significant.

Immunocytochemical analyses. Cultured cells were washed twice with PBS(−), fixed in 4% paraformaldehyde solution for 60 minutes at room temperature, and rendered permeable with PBS(−) containing 0.1% Triton X-100 for 1.5 minutes. Prior to the primary antibody reaction, cells were covered with blocking solution (3% bovine serum albumin (BSA) in PBS(−)) for 60 minutes to block nonspecific antibody binding. Then the cells were incubated with antibodies to human NMU protein. Antibodies were stained with a goat anti-rabbit secondary antibody conjugated to rhodamine (Cappel, Durham, NC) for revealing endogenous NMU, and viewed with a microscope (DP50; Olympus, Tokyo, Japan).

RNA interference assay. We had previously established a vector-based RNA interference (RNAi) system, psiH1BX3.0, to direct the synthesis of short interfering RNAs (siRNA) in mammalian cells (6, 7, 10, 11). We transfected

10 μg of siRNA expression vector, using 30 μL of LipofectAMINE 2000 (Invitrogen), into NSCLC cell lines A549 and LC319, both of which overexpressed *NMU, GHSR1b, NTSR1*, and *FOXM1* endogenously. The transfected cells were cultured for 5 days in the presence of appropriate concentrations of geneticin (G418), after which, cell numbers and viability were measured by Giemsa staining and triplicate 3-(4,5-dimethylthiazol-2-yl)-2,5-diphenyltetrazolium bromide (MTT) assays. The target sequences of the synthetic oligonucleotides for RNAi were as follows: control 1 [*EGFP*: enhanced green fluorescent protein gene, a mutant of *Aequorea victoria* green fluorescent protein], 5′-GAAGCAGCACGACTTCTTC-3′; control 2 (Luciferase: *Photinus pyralis* luciferase gene), 5′-CGTACGCGGAATACTTCGA-3′; control 3 (Scramble: chloroplast *Euglena gracilis* gene coding for 5S and 16S rRNAs), 5′-GCGCGCTTTGTAGGATTCG-3′; siRNA-NMU (si-*NMU*), 5′-GAGATTCAGAGTGGACGAA-3′; siRNA-GHSR-1 (si-*GHSR-1*), 5′-CCTCTACCTGTCCAGCATG-3′; siRNA-GHSR-2 (si-*GHSR-2*), 5′-GCTGGTCATCTTCGTCATC-3′; siRNA-NTSR1-1 (si-*NTSR1-1*), 5′-GTTCATCAGCGCCATCTGG-3′; siRNA-NTSR1-2 (si-*NTSR1-2*), 5′-GGTCGTCATACAGGTCAAC-3′. To validate our RNAi system, individual control siRNAs (EGFP, Luciferase, and Scramble) were initially confirmed using semiquantitative RT-PCR to decrease the expression of the corresponding target genes that had been transiently transfected into COS-7 cells. Down-regulation of *NMU, GHSR1b*, and *NTSR1* expression by their respective siRNAs (si-*NMU*, si-*GHSR-1*, si-*NTSR1-1*, and si-*NTSR1-2*), but not by controls, was confirmed with semiquantitative RT-PCR in the cell lines used for this assay.

NMU-expressing COS-7 transfectants. NMU-expressing stable transfectants were established according to a standard protocol. The entire coding region of *NMU* was amplified by RT-PCR using the primer sets described above. The product was digested with *Bam*HI and *Xho*I, and cloned into appropriate sites of a pcDNA3.1-myc/His A(+) vector (Invitrogen) that contained c-myc-His-epitope sequences (LDEESILKQEHHHHHH) at the COOH-terminal of the NMU protein. Using FuGENE 6 Transfection Reagent (Roche Diagnostics, Basel, Switzerland) according to the manufacturer's instructions, we transfected COS-7 cells, which do not express endogenous NMU, with plasmids expressing either *NMU* (pcDNA3.1-*NMU*-myc/His), an antisense strand of *NMU* (pcDNA3.1-antisense), or mock plasmids (pcDNA3.1). Transfected cells were cultured in DMEM containing 10% FCS and geneticin (0.4 mg/mL) for 14 days; then 50 individual colonies were trypsinized and screened for stable transfectants by a limiting-dilution assay. Expression of NMU was determined in each clone by RT-PCR, Western blotting, and immunostaining.

Cell growth and colony formation assays. COS-7 transfectants that stably expressed NMU were seeded onto six-well plates (5×10^4 cells/well), and maintained in medium containing 10% FCS and 0.4 mg/mL geneticin for 24, 48, 72, 96, 120, and 144 hours. At each time point, cell proliferation was evaluated by the MTT assay using Cell Counting Kits (Wako, Osaka, Japan). Colonies were counted at 144 hours. All experiments were done in triplicate. Interaction of NMU-25 with COS-7 cells were examined by flow cytometric analysis. Briefly, subconfluent cells were harvested in Cell Dissociation Solution (Sigma-Aldrich) and suspended in DMEM. Then, 1×10^6 cells/microtube were washed with assay buffer [PBS(−) with 10 mmol/L $MgCl_2$, 2 mmol/L EDTA, and 0.1% BSA], and the cells were incubated with 0.5 to 10 μmol/L of rhodamine-labeled NMU-25 peptide (NMU-25-rhodamine; Phoenix Pharmaceuticals, Inc., Belmont, CA) in assay buffer for 2 hours at room temperature. Subsequently, the cells were washed twice with assay buffer. To detect the population of cells binding to rhodamine-labeled NMU-25, flow cytometry was done using a Becton Dickinson FACSCalibur and analyzed by Cell Quest software.

Ligand receptor binding assay. To confirm binding of NMU-25 to the endogenous candidate receptors on the NSCLC cells, we did a receptor-ligand binding assay using the LC319 and PC14 cells that expressed GHSR1b and NTSR1, but did not express NMU1R and NMU2R. Briefly, the trypsinized cells were seeded onto 96-well (with a black wall and clear bottom) microtiter plates 24 hours prior to the assay. The medium was removed and the cells were incubated with Cy5-labeled NMU-25 peptide (1 μmol/L) with or without a 10-fold excess of unlabeled NMU-25 peptide as a competitor. The plate was incubated in the dark for 24 hours at 37°C and was then scanned on the 8200 Cellular Detection System (Applied Biosystems, Foster City, CA) to quantify the amount of Cy5 fluorescence probe bound to the surface of each cell.

Immunocytochemistry for internalized receptors. To investigate the association of NMU-25 with its candidate receptors, GHSR1b and NTSR1, we did the following experiments. The entire coding region of each receptor gene was amplified by RT-PCR using primers *GHSR1b* (5′-GGAATTCCATGTGGAACGCGACGCCCAGCGAA-3′ and 5′-CGCGGATCCGCGGAGAGAAGGGAGAAGGCACAGGGA-3′) and *NTSR1* (5′-GGAATTCCATGCGCCTCAACAGCTCCGCGCCGGGAA-3′ and 5′-CGCGGATCCGCGGTACAGCGTCTCGCGGGTGGCATTGCT-3′). The products were digested with *Eco*RI and *Bam*HI and cloned into appropriate sites of p3XFLAG-CMV10 vector (Sigma-Aldrich). We transfected COS-7 cells with FLAG-tagged GHSR1b or NTSR1 expression plasmids using FuGENE 6 Transfection Reagent, as described above. The cells subjected to internalization assays were exposed to NMU-25 (10 μmol/L) for 120 minutes. Cells were then fixed with 4% paraformaldehyde solution for 15 minutes at 37°C, and washed with PBS(−). Specimens were incubated in PBS(−) containing 0.1% Triton X-100 for 10 minutes and subsequently washed with PBS(−). Prior to the primary antibody reaction, cells were incubated in CAS-BLOCK (Zymed Laboratories, Inc., South San Francisco, CA) for 10 minutes to block nonspecific antibody binding. Then the cells were incubated with both rabbit polyclonal anti-GHSR antibody and goat polyclonal anti-NTSR1 antibody. Antibodies were stained with both anti-rabbit secondary antibody conjugated to Alexa Fluor 488 (Molecular Probes, Eugene, OR) and anti-goat secondary antibody conjugated to Alexa Fluor 594 (Molecular Probes). DNA was stained with 4′,6-diamidino-2-phenylindole (DAPI). Images were viewed and assessed using a confocal microscopy (TCS SP2 AOBS; Leica Microsystems, Wetzlar, Germany).

Internalization study with fluorescence ligand of NMU. LC319 cells were grown in DMEM containing 10% FCS. The cells were washed in PBS(−), and preincubated for 10 minutes at 37°C in DMEM containing 0.1% BSA. They were then incubated for various periods of time with Alexa Fluor 594–labeled NMU-25 peptide in DMEM containing 0.1% BSA. At the end of the incubation, the cells were washed thrice with ice-cold PBS(−), fixed with 4% paraformaldehyde solution, initially for 5 minutes on ice, and then for 15 minutes at room temperature. The cells were washed and treated with DAPI. Images were viewed and assessed using a confocal microscopy (TCS SP2 AOBS; Leica Microsystems). Optical sections with intervals of 0.25 μm were taken with a 63×/1.4 objective.

Detection of receptor dimerization. Cultured cells were washed twice with ice-cold PBS(−) and incubated with 5 mmol/L dithiobis[succinimidyl-propionate] (Pierce, Rockford, IL) for 60 minutes in PBS(−) on ice. The reaction was quenched by incubation with Stop solution [1 mol/L Tris (pH 7.5)] in a final concentration of 50 mmol/L Tris for 15 minutes on ice. Cells were then washed twice with ice-cold PBS(−) and lysed in ice-cold Tx/G buffer [300 mmol/L NaCl, 1% Triton X-100, 10% glycerol, 1.5 mmol/L $MgCl_2$, 1 mmol/L $CaCl_2$, and 10 mmol/L iodoacetamide in 50 mmol/L Tris-Cl (pH 7.4)] containing protease inhibitor (Protease Inhibitor Cocktail Set III; Calbiochem) for 60 minutes on ice. Iodoacetamide was included in each buffer used for protein preparation to prevent nonspecific disulfide linkages. The lysates were then centrifuged for 15 minutes at 15,000 rpm at 4°C, and the supernatants were incubated with anti-FLAG M2-agarose affinity beads (Sigma-Aldrich) at 4°C overnight. The immunoprecipitates (containing cell surface receptors) were collected, washed thrice with TBST buffer [150 mmol/L NaCl, 0.05% Tween 20 in 20 mmol/L Tris-Cl (pH 7.6)], and eluted in non–reducing Laemmli sample buffer. The solutions were subjected to SDS-PAGE, and receptor proteins were detected by Western blot analysis using a mouse monoclonal anti-FLAG M2 antibody, goat polyclonal anti-NTSR1 antibody, or rabbit polyclonal anti-GHSR antibody as a primary antibody, and rec-Protein G-Peroxidase Conjugate (Zymed Laboratories) to detect antigen-antibody complexes.

Measurement of cyclic AMP levels. Trypsinized LC319 cells were seeded onto 96-well microtiter plate (5.0×10^4 cells) and cultured in appropriate medium supplemented with 10% FCS for 24 hours, and then the medium was changed to serum-free/1 mmol/L of 3-isobutyl-1-methylxanthine 20 minutes prior to the assay. Next, cells were incubated with individual concentrations of peptides (NMU-25, GHRL, or NTS) for

20 minutes and their cyclic AMP (cAMP) levels were measured using the cAMP EIA System (GE Healthcare Bio-Sciences).

Identification of downstream genes of NMU by cDNA microarray. LC319 cells were transfected with either siRNA against *NMU* (si-*NMU*) or Luciferase (LUC; control siRNA). mRNAs were extracted 0, 6, 12, 24, 36, 48, and 60 hours after the transfection, labeled with Cy5 or Cy3 dye, and subjected to cohybridization onto cDNA microarray slides containing 32,256 genes as described (5). After normalization of the data, genes with signals higher than the cutoff value were analyzed further. Genes whose intensity was significantly decreased in accordance with the reduction of *NMU* expression were initially selected using self-organizing map cluster analysis (22). Validation of candidate downstream genes of NMU was done using semiquantitative RT-PCR experiments of the same mRNAs from LC319 cells used for microarray hybridization, with gene-specific primers.

Results

NMU in lung tumors and normal tissues. To search for novel target molecules for the development of therapeutic agents and/or diagnostic biomarkers for NSCLC, we first screened genes that showed 5-fold higher expression in >50% of 37 NSCLCs analyzed by cDNA microarray. Among the 23,040 genes screened, we identified the *NMU* transcript to be frequently overexpressed in these NSCLCs and confirmed increased *NMU* expression in the majority of additional NSCLC cases (Fig. 1*A*). In addition, we observed the up-regulation of *NMU* in 13 of 15 NSCLC cell lines and in all 4 SCLC cell lines examined (Fig. 1*B*). Using immunoblot analyses, we subsequently confirmed the expression of NMU protein in lung cancer tissues and cell lines. Western blot analysis revealed an increased NMU protein expression in tumor tissues from the representative pairs of NSCLC samples analyzed (Supplementary Fig. S1*A*). We also found increased NMU protein expression in lung cancer cell lines (Supplementary Fig. S1*B*); the results were consistent with the RT-PCR data (Fig. 1*B*). Northern blotting with *NMU* cDNA as a probe identified a 0.8 kb transcript as a very weak band only in brain and stomach among the 15 normal human tissues examined (data not shown). We also examined NMU expression in clinical lung cancers using tissue microarray system. Positive staining (dark brown staining in >50% of tumor cells completely obscuring the cytoplasm) was observed in 68% of surgically resected NSCLCs (220 of 326) and 82% of SCLCs (14 of 17), whereas no staining was observed in any of normal lung tissues examined (Fig. 1*C*). Positive staining was also observed in all of three large cell neuroendocrine carcinomas. The positive signal by anti-NMU antibody obtained in lung cancer tissues was completely diminished by preincubation of the antibody with recombinant human NMU, indicating its high specificity to NMU protein (Supplementary Fig. S1*C*). We found that patients with NSCLC with NMU-positive tumors showed shorter survival times than patients whose tumors were negative for NMU (P = 0.0363 by the log-rank test; Fig. 1*D*). By univariate analysis, pT (T_1 versus $T_{2\text{-}4}$), pN (N_0 versus $N_{1\text{-}2}$), age (<65 versus ≥65), gender (female versus male), and NMU expression (negative versus positive) were all significantly related to poor survival among patients with NSCLC (P = 0.0012, < 0.0001, 0.0024, 0.0237, and 0.0379, respectively). In multivariate analysis of the prognostic factors, only pT stage, pN stage, gender, and age were indicated to be an independent prognostic factor (P = 0.0011, < 0.0001, 0.0495, and 0.0007, respectively), whereas NMU expression could not be an independent factor (P = 0.0909), thus suggesting the relevance of NMU expression in tumor cells to these clinicopathologic factors.

Effect of NMU on the growth of NSCLC cells. To assess whether NMU is essential for the growth or survival of lung cancer cells, we

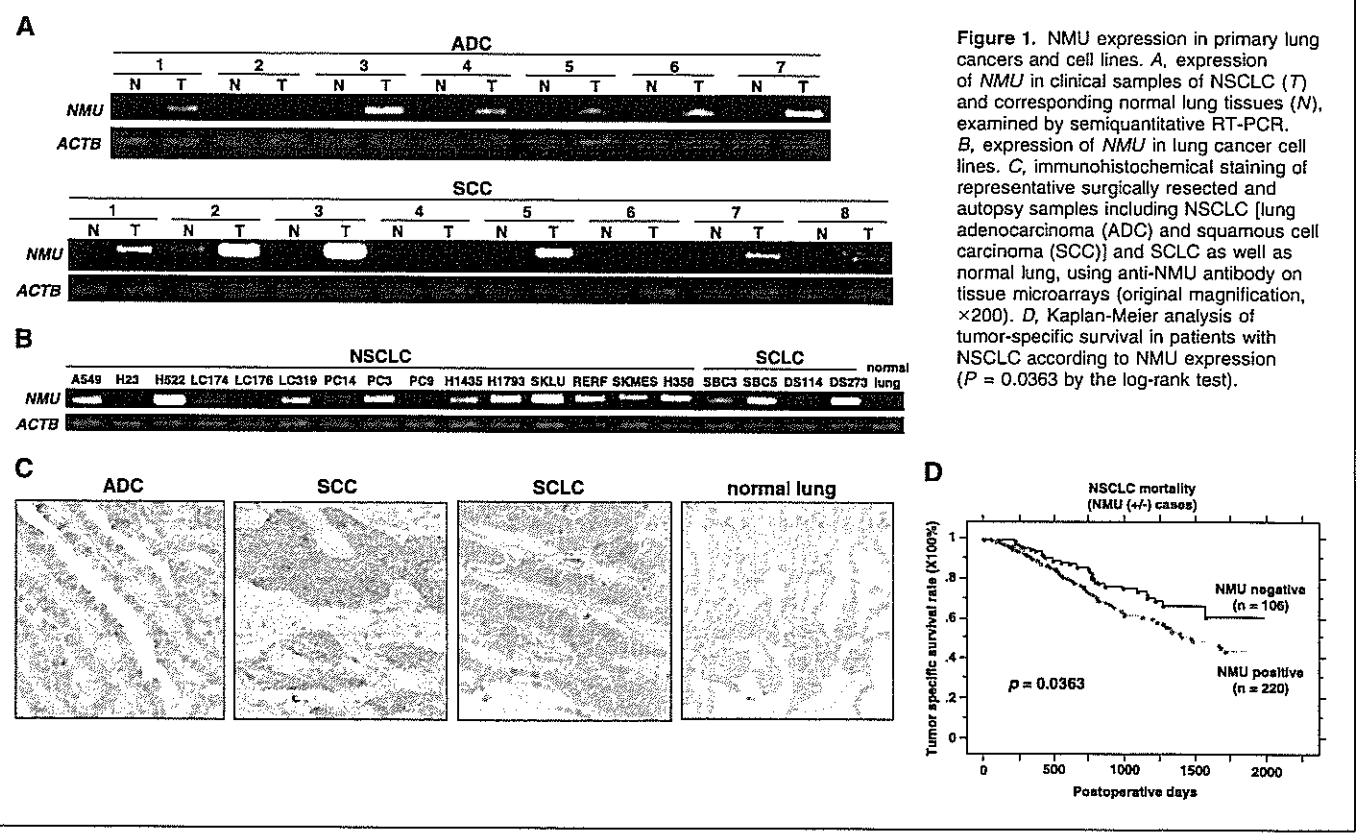

Figure 1. NMU expression in primary lung cancers and cell lines. *A*, expression of *NMU* in clinical samples of NSCLC (*T*) and corresponding normal lung tissues (*N*), examined by semiquantitative RT-PCR. *B*, expression of *NMU* in lung cancer cell lines. *C*, immunohistochemical staining of representative surgically resected and autopsy samples including NSCLC [lung adenocarcinoma (ADC) and squamous cell carcinoma (SCC)] and SCLC as well as normal lung, using anti-NMU antibody on tissue microarrays (original magnification, ×200). *D*, Kaplan-Meier analysis of tumor-specific survival in patients with NSCLC according to NMU expression (P = 0.0363 by the log-rank test).

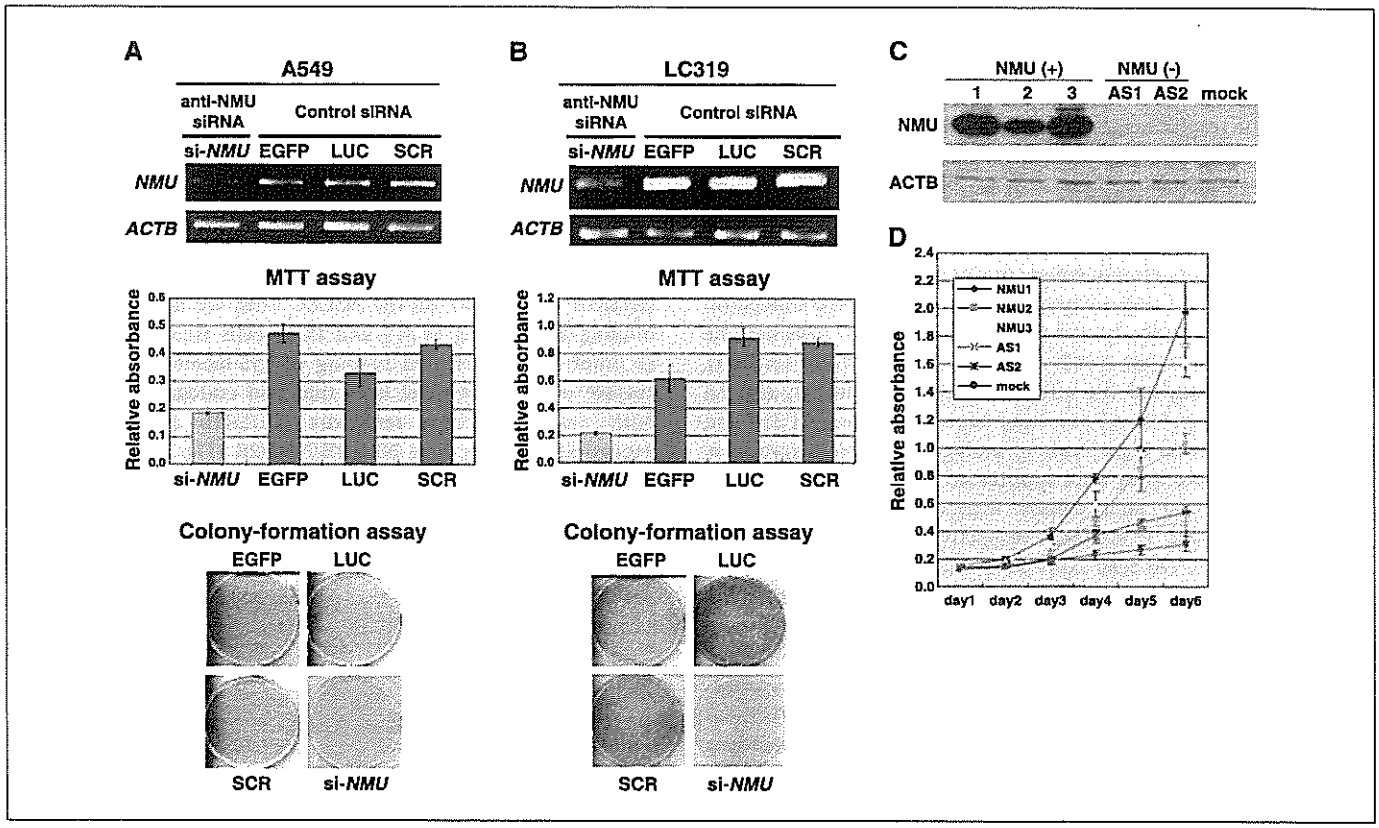

Figure 2. Growth effect of NMU. *A* and *B*, expression of *NMU* in response to si-*NMU* or control siRNAs (EGFP, LUC, or SCR) in A549 (*A*) and LC319 (*B*) cells, analyzed by semiquantitative RT-PCR (*A* and *B*, *top*). Viability of A549 or LC319 cells evaluated by MTT assay in response to si-NMU, -EGFP, -LUC, or -SCR (*A* and *B*, *middle*). Colony formation assays of A549 and LC319 cells transfected with specific siRNAs or control plasmids (*A* and *B*, *bottom*). All experiments were done in triplicate. *C* and *D*, effect of NMU on the growth of COS-7 cells. Expression of NMU in stable transfectants of COS-7 cells on Western blots (*C*). Three independent transfectants expressing high levels of NMU (COS-7-NMU-1, -2, and -3) and controls (COS-7-AS1, -AS2, and mock) were each cultured in triplicate; at each time point, the cell viability was evaluated by the MTT assay (*D*).

designed and constructed plasmids to express siRNA against *NMU* (si-*NMU*), and three different control plasmids [siRNAs for EGFP, Luciferase (LUC), or Scramble (SCR)], and transfected them into A549 (Fig. 2*A*) and LC319 (Fig. 2*B*) cells to suppress the expression of endogenous *NMU*. The amount of *NMU* transcript in the cells transfected with si-*NMU* was significantly decreased in comparison with cells transfected with any of the three control siRNAs (Fig. 2*A* and *B*, *top*); transfection of si-*NMU* also resulted in significant decreases in cell viability and colony numbers measured by MTT and colony formation assays (Fig. 2*A* and *B*, *middle* and *bottom*).

Autocrine growth-promoting effect of NMU. To disclose the potential role of NMU in tumorigenesis, we prepared plasmids designed to express either *NMU* (pcDNA3.1-*NMU*-myc/His) or a complementary strand of *NMU* (pcDNA3.1-antisense). We transfected each of these two plasmids into COS-7 cells and confirmed the expression of NMU protein in cytoplasm and Golgi structures by immunocytochemical staining using anti-NMU antibody (data not shown).

To determine the effect of NMU on the growth of mammalian cells, we carried out a colony formation assay of COS-7-derived transfectants that stably expressed NMU. Immunocytochemical analysis using anti-NMU antibody detected NMU protein in >90% of the COS-7 cells in the culture (Supplementary Fig. S2*A*). We established three independent COS-7 cell lines expressing exogenous NMU (COS-7-NMU-1, -2, and -3; Fig. 2*C*), and compared their growth with control cells transfected with antisense strand or mock vector (COS-7-AS-1 and -2; COS-7-mock). Growth of all of the three COS-7-NMU cells was promoted at a significant degree in accordance with the expression level of NMU (Fig. 2*D*). There was also a remarkable tendency in COS-7-NMU cells to form larger colonies than the control cells (Supplementary Fig. S2*B*). Furthermore, we did colony formation assays to investigate whether the NMU could act as a growth-promoting factor for lung-cancer cells (LC319). The number of geneticin-resistant colonies was significantly increased in dishes containing LC319 cells that had been transfected with the sense strand of cDNA (pcDNA3.1-*NMU*-myc/His) corresponding to the normal transcript, in comparison to cells transfected with the mock vector (Supplementary Fig. S2*C*).

As the immunohistochemical analysis on tissue microarray had indicated that lung cancer patients with NMU-positive tumors showed shorter cancer-specific survival periods than patients whose tumors were negative for NMU, we did Matrigel invasion assays using COS-7-NMU cells. Invasion of COS-7-NMU cells through Matrigel was significantly enhanced, compared with the control cells transfected with mock plasmids, suggesting that NMU could also contribute to the highly malignant phenotype of lung cancer cells (Supplementary Fig. S2*D*).

Subsequently, we carried out autocrine assays using the active form of a 25–amino acid polypeptide of commercially available NMU (NMU-25). To investigate whether NMU-25 would affect cell growth, we incubated COS-7 cells with either NMU-25 or BSA (control) at final concentrations of 0.3 to 15 μmol/L in the culture medium. COS-7 cells incubated with NMU-25 showed enhancement of the cell

growth by MTT and colony formation assays, compared with the control, in a dose-dependent manner (Fig. 3*A* and *B*). We also detected by flow cytometry that rhodamine-labeled NMU-25 peptide bound to the surface of COS-7 cells in a dose-dependent manner (Fig. 3*C*). The results suggested that the growth-promoting effect of NMU was likely to be mediated through binding of NMU-25 to a receptor(s) on the cell surface of COS-7. Subsequently, we investigated whether anti-NMU antibody (0.5-7.5 μmol/L) could inhibit the growth of COS-7 cells cultured in medium containing 3 μmol/L of NMU-25. Expectedly, growth enhancement caused by the addition of 3 μmol/L of NMU-25 was neutralized by the 7.5 μmol/L concentration of anti-NMU antibody, and the viability of COS-7 cells became almost equivalent to that of cells cultured without NMU-25 (Fig. 3*D*).

We then investigated the effect of anti-NMU antibody (0.5-7.5 μmol/L) on the growth of two lung cancer cell lines, LC319 and A549, which showed high levels of endogenous *NMU* expression. The growth of both lines were suppressed by the addition of anti-NMU antibody into their culture media, in a dose-dependent manner ($P < 0.0001$, $P = 0.0002$, respectively; each paired t test), whereas that of LC176 cells expressing NMU at a hardly detectable level was not affected (Supplementary Fig. S3). These data indicated that NMU functions as an autocrine/paracrine growth factor for the proliferation of NSCLC cells.

GHSR1b/NTSR1 as receptors for NMU in a growth-promoting pathway. Two known NMU receptors, NMU1R (FM3/GPR66) and NMU2R (FM4), play important roles in energy homeostasis (17–19). NMU1R is present in many peripheral human tissues (17–19), but NMU2R is only located in the brain. To investigate whether *NMU1R* and *NMU2R* genes were expressed in NSCLCs and whether it is responsible for the growth-promoting effect, we analyzed the expression of these NMU receptors in normal human brain and lung, in NSCLC cell lines, and in clinical tissues by semiquantitative RT-PCR experiments. Neither *NMU1R* nor *NMU2R* expression was detected in any of the lung cancer cell lines or clinical cancer samples examined, although *NMU1R* was expressed in the lung and *NMU2R* in the brain (data not shown), suggesting that NMU is likely to mediate its growth-promoting effect through interaction with other receptor(s) in lung cancer cells.

NMU1R and NMU2R were originally isolated as homologues of known neuropeptide GPCRs. We speculated that unidentified NMU receptor(s) having some degree of homology to NMU1R/NMU2R would be involved in the signaling pathway and searched for candidate NMU receptors using the BLAST program. The homology and expression patterns of genes in NSCLCs in our expression profile data picked up GHSR1b and NTSR1 as good candidates. GHSR has two transcripts, types 1a and 1b. The human GHSR type 1a cDNA encodes a predicted polypeptide of 366 amino acids with seven transmembrane domains, a typical feature of G protein–coupled receptors. A single intron separates its open reading frame into two exons encoding transmembrane domains 1 to 5 and 6 to 7, placing GHSR1a into the intron-containing class of GPCRs. Type 1b is a nonspliced mRNA variant transcribed from a single exon that encodes a polypeptide of 289 amino acids with five transmembrane domains. Our semiquantitative RT-PCR analysis using specific primers for each variant indicated that *GHSR1a* was not expressed in NSCLCs. On the other hand, *GHSR1b* and *NTSR1* were expressed at a relatively high level in some NSCLC cell lines, but not in normal lung (Fig. 4*A*). The *GHSR1b* product reveals 46% homology to NMU1R, and *NTSR1* encodes 418 amino acids with 47% homology to NMU1R. COS-7 cells examined using the autocrine growth-promoting effect of NMU as described above, were confirmed by semiquantitative RT-PCR analysis to endogenously express both *GHSR1b* and *NTSR1* (data not shown). Furthermore, we did immunohistochemical analysis with anti-GHSR1b and anti-NTSR1 polyclonal antibodies using tissue microarrays consisting of 326 NSCLC tissues. Of the 326 cases, GHSR1b staining was positive for 218 (67%; Fig. 4*B, top*), and 217 cases were positive for NTSR1 (67%; Fig. 4*B, bottom*). The expression pattern of GHSR1b or NTSR1 was significantly concordant with NMU expression in these tumors ($\chi^2 = 68$ and 79; $P < 0.0001$ and <0.0001, respectively).

To investigate the binding of NMU-25 to the endogenous GHSR1b and NTSR1 on the NSCLC cells, we did receptor-ligand binding assay using LC319 and PC14 cells treated with NMU-25 (1 μmol/L). We detected binding of Cy5-labeled NMU-25 to the surface of these two cell lines that had endogenously expressed both novel candidate receptors (GHSR1b and NTSR1), but expressed no detectable NMU1R/NMU2R (Fig. 4*A*). The binding activity was elevated in a dose-dependent manner (data not

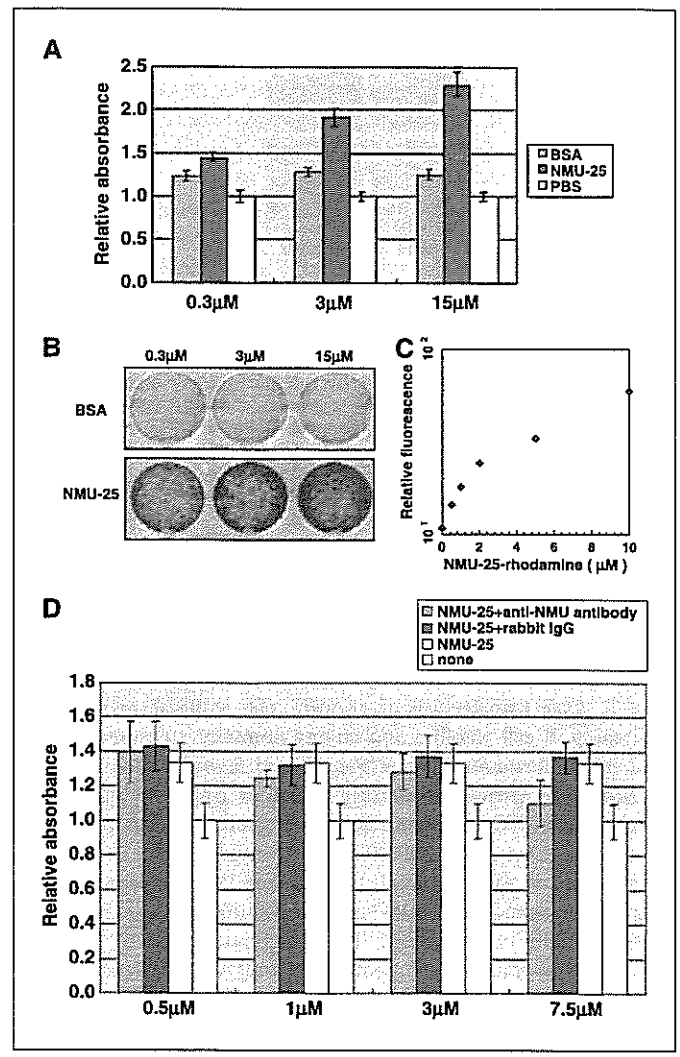

Figure 3. Autocrine effect of NMU on growth of mammalian cells. *A* and *B*, cell viability (*A*) and numbers (*B*) counted by MTT and colony formation assays (COS-7 cells treated with NMU-25 in final concentrations of 0.3-15 μmol/L). *C*, flow cytometric analysis detecting the levels of rhodamine-labeled NMU-25 peptide bound to the surface of COS-7 cells (0-10 μmol/L; *y* axis). *D*, MTT assay evaluating the competitive-binding effect of anti-NMU antibody (0.5-7.5 μmol/L; *y* axis) on the activity of NMU-25 peptide (3 μmol/L) in the culture medium of COS-7 cells.